12-2013

Assessing the Impact of Chlorine Residual on Trihalomethane and Haloacetonitrile Formation Under Chlorination and Chloramination Disinfection Regimes

Thien Duc Do
University of Arkansas, Fayetteville

Assessing the Impact of Chlorine Residual on Trihalomethane and Haloacetonitrile Formation Under Chlorination and Chloramination Disinfection Regimes

Assessing the Impact of Chlorine Residual on Trihalomethane and Haloacetonitrile Formation Under Chlorination and Chloramination Disinfection Regimes

A thesis submitted in partial fulfillment
of the requirements for the degree of
Master of Science in Environmental Engineering

by

Thien Duc Do
Ho Chi Minh City University of Technology
Bachelor of Science in Environmental Engineering, 2010

December 2013
University of Arkansas

This thesis is approved for recommendation to the Graduate Council.

_____
Dr. Julian Fairey
Thesis Director

_____
Dr. Wen Zhang
Committee Member

_____
Dr. Ashley Pifer
Committee Member

Abstract

A disinfection byproduct (DBP) formation potential (FP) test can be used to indirectly measure the concentration of DBP precursors in natural waters, permitting assessment of various DBP-related treatment processes and control strategies. While these tests require a 7-day chlorine residual (CR) between 3-5 mg L^{-1} as Cl_2, it is not well known if this recommended residual corresponds to the true DBPFP (i.e., the maximum concentrations) for trihalomethanes (THMs) and haloacetonitriles (HANs). In this study, THMs and HANs were quantified as a function of CR under three common disinfection regimes: (1) free chlorine at pH 7.0 (FC7), (2) monochloramine at pH 7.0 (MC7), and (3) monochloramine at pH 8.3 (MC8). Three source waters were collected, one from a drinking water source (LW) and two from the effluent of a wastewater treatment plant (WW1 and WW2), and used to generate a total of 90 sample waters for the DBPFP experiments. Trichloromethane (TCM) was the predominant THM formed in the sample waters, and, for MC8, achieved its maximum value of ~40 µg L^{-1} at a CR of 30 mg L^{-1} as Cl_2 (referred to as CR_{MAX}), and in excess of the 3-5 mg L^{-1} as Cl_2 target residual. For the FC7 and MC7 disinfection regimes, TCM concentrations continued to increase beyond the maximum CR achieved in this study (73.6- and 17.1 mg L^{-1} as Cl_2, respectively), indicating its true FP was not reached. CR_{MAX} values for the bromine-substituted THMs and HANs varied by disinfectant type and pH, however none were between the 3-5 mg L^{-1} as Cl_2 recommended residual, and were limited by the low bromide concentrations in the source waters (< 0.24 mg L^{-1}). For dichloroacetonitrile, the predominant HAN formed, the CR_{MAX} was 1.5-1.7 mg L^{-1} as Cl_2 for FC7 and in excess of 15 mg L^{-1} as Cl_2 for MC7 and MC8. The results of this study demonstrate the impact of CR on the formation of THMs and HANs, and can be leveraged to help assess various DBP-precursor removal processes and be used to guide development of more a more robust DBPFP test.

Contents

List of Tables

List of Figures

Abbreviations

BSF – bromine substitution factor;

DBAN – dibromoacetonitrile;

DBP – disinfection byproduct;

DBPFP – DBP formation potential;

DCAN – dichloroacetonitrile;

DBCM – dibromochloromethane;

DCBM – dichlorobromomethane;

FC7 – free chlorine at pH 7.0;

LW – Beaver Lake water collected on 08/28/13;

MC7 – monochloramine at pH 7.0;

MC8 – monochloramine at pH 8.3;

TBM – bromoform;

TCM – trichloromethane;

TotDXBr – total bromine in DCBM and DBCM;

WW1 – Noland wastewater effluent collected on 7/27/13;

WW2 – Noland wastewater effluent collected on 9/19/13;

1. Introduction

Water utilities add disinfectants, such as chlorine, to drinking water to protect the public from disease outbreaks caused by pathogens. Disinfectants, however, can react with natural organic matter (NOM) to form disinfection byproducts (DBPs), some of which are associated with adverse health outcomes (Rook, 1976). In 1979, the US Environmental Protection Agency (USEPA) regulated the sum total of four trihalomethanes (THM4) in finished drinking water at 100 μg L^{-1}. Under the *Stage 1 Disinfectants and Disinfection Byproducts Rule* (D/DBPR) (USEPA, 1999), the *Maximum Contaminant Level* (MCL) for THM4 was lowered to 80 μg L^{-1}. Compliance with the Stage 1 D/DBP rule with regard to THM4 was based on a distribution system-wide running annual average. Under this rule, water utilities could offset THM4 values that were higher than the MCL, typically found in the far reaches of the distribution system, with lower concentrations found at other sampling points. However, under the Stage 2 D/DBPR (USEPA, 2006), while the THM4 MCL remained at 80 μg L^{-1}, compliance is based on locational running annual averages. As such, to achieve compliance under this new (and current) rule, each sampling point within the distribution system must have an annual average less than 80 μg L^{-1}. This change in the regulations has caused water utilities to seek additional THM4 control strategies.

While free chlorine (HOCl and OCl^-) is the most common drinking water disinfectant used in the United States and worldwide, monochloramine (NH_2Cl) has gained popularity to curb THM4 formation, especially as a secondary disinfectant (Seidel et al., 2005). In addition to water utilities switching disinfectants, drinking water sources are becoming increasingly impacted by wastewater effluents, which are typically enriched in organic nitrogen-containing compounds. As a result of these disinfectant and source water changes, groups of nitrogen-containing DBPs, such as haloacetonitriles (HANs), may form at higher concentrations in distribution systems. However, it is important to note that although HANs are more toxic than regulated DBPs (Muellner et al., 2007), they are not presently regulated by the USEPA.

Assessing the impact of switching secondary disinfectants on DBP formation is complicated by several factors, including the (1) variability in NOM quantity and characteristics over time, (2) changes in NOM removal within the drinking water treatment plant (DWTP), (3) disinfectant type and dose, and (3) pH of disinfection and particle removal processes. A lack of control of any of these factors can result in an

improper assessment of the benefits gained from a given DBP control strategy or precursor removal process. A common way to indirectly measure DBP precursors is to perform a DBP formation potential (DBPFP) test. As described in *Standard Methods (SM) for the Examination of Water & Wastewater* (Eaton, 2005), trihalomethane formation potential (THMFP) can be measured by following SM5710 B and, for other DBPs like HANs, by SM5710 D. These methods specify a disinfectant residual (e.g., free chlorine or monochloramine) of 3-5 mg L^{-1} as Cl_2 following a 7-day reaction time at room temperature in the absence of light. The formation potential tests are designed to indirectly measure the concentrations of DBP precursors. However, very limited research is available evaluating the effect of chlorine residual (CR) on DBPFP under various disinfection regimes, and thus it is not known whether the true formation potential is being assessed.

In this study, we analyzed the effect of CR on THM4 and HAN formation under three disinfection regimes: free chlorine at pH 7.0 (FC7), monochloramine at pH 7.0 (MC7), and monochloramine at pH 8.3 (MC8). The objective of this study was to determine the CRs at which the maximum THM4 and HAN formation occurred. Chlorination and chloramination experiments were performed using three untreated source waters, including two wastewater effluents and one lake water. The wastewater effluents were selected because they were enriched with organic carbon and organic nitrogen, both precursors of DBPs. THM4 and HANs were quantified as a function of CR under the three disinfection regimes and compared to the Standard Methods definition of formation potential. To develop a technique to rapidly assess DBPFP, correlations were sought between previously developed spectrophotometric metrics (Pifer and Fairey, 2012; Granderson et al., 2013) and THM and HAN formation to determine the accuracy of the precursor surrogate parameters. The information developed in this study could be used to improve the assessment of strategies used to remove THM4 and HAN precursors at DWTPs, and guide subsequent development of formation potential tests for non-halogenated DBPs, such as nitrosamines.

2. Materials and methods

2.1 Chemicals and materials

All chemicals used to prepare standards and reagents were ACS grade and were made in Milli-Q water (18.2 MΩ-cm), generated using a Millipore Integral 3 purification system. Ammonium chloride

(granular) was dehydrated at 105°C for at least 8 hours prior to use as an ammonium source for the monochloramine and ammonium standards. Sodium sulfate (granular, anhydrous) was purified at 400°C for at least 30 minutes prior to use as the extracting salt following EPA 551.1.

Glassware and plastic-ware were cleaned rigorously with a mixture of Alconox soap and tap water and rinsed thoroughly with deionized water and Milli-Q water. Drying procedures were as follows: glass vials were baked at 400°C for at least 30 minutes, volumetric flasks were air-dried at room temperature, PTFE-lined lids were rinsed with acetone and baked at 80°C, HDPE carboys were baked at 40°C for at least 8 hours, and 0.7-µm glass fiber filters (GFFs) and 0.45 µm polyethersulfone (PES) membranes were rinsed prior to use with 1-L and 0.5-L of Milli-Q water, respectively. Following the first round of DBPFP experiments (see Section 2.3), all glassware and pipette tips were soaked in a solution of 100 mg/L as Cl_2 water for 24 hours to reduce their chlorine demand before being rinsed with Distilled De-Ionized (DDI) water. Thereafter, the glassware were baked at 400°C for at least 30 minutes while the pipette tips were baked at 40°C for at least 8 hours.

2.2 Site description

Water samples for this study were collected from two sites – one WWTP effluent and one drinking water source. The WWTP effluent was collected from the Paul R. Noland WWTP in Fayetteville, AR. This WWTP was designed to handle Fayetteville's current treatment requirements and anticipated population growth through 2020 with an average daily flow of 12.6 million gallons per day (MGD), a maximum daily flow of 29 MGD, and a maximum monthly flow of 17 MGD. The Noland WWTP has secondary biological treatment including anoxic-aerobic basins for nutrient removal, and tertiary treatment including UV-disinfection. The other water source was Beaver Lake, which is treated by Beaver Water District (BWD) to supply drinking water to the approximately 500,000 residents of Northwest Arkansas. Additional information about Beaver Lake and the raw water quality has been described previously (Pifer and Fairey, 2012).

2.3 Source water handling and collection

Source waters were collected in 9-L HDPE carboys from Noland WWTP effluent and from the BWD intake structure for use in the DBPFP experiments. Effluent water was collected on 7/24/13 (WW1) and 9/19/13 (WW2) and lake water was collected on 8/28/13 (LW). For each source water, a set of DBPFP experiments was performed as described in Section 2.4. As such, the first set of experiments was done with WW1, the second with LW, and the third with WW2. To reduce the filtration time, samples were pre-filtered with 0.7-µm GFFs prior to filtration with 0.45-µm PES membranes and stored at 4°C in the dark until use.

2.4 Water quality tests

Filtered raw water pH, Dissolved Organic Carbon (DOC), Ultraviolet Absorbance (UVA) spectra (at 225 to 600 nm), fluorescence excitation-emission matrices (EEMs) and total ammonia were measured. The EEMs were collected at excitation wavelengths between 225-400 nm and emission wavelengths of 260-600 nm. The methods used to measure these parameters (with an exception of total ammonia) were described elsewhere (Pifer and Fairey, 2012)

Total ammonia was measured using an ammonia electrode (Thermo Orion 9512, Waltham, MA) connected to an Accumet XL60 meter. The method entitled "*Measuring Ammonia in Solutions that Wet the Membrane*" (Thermo-Scientific) was used because the wastewater effluent was thought to have the surfactant that wets the membrane. 1 mL of pH adjusting reagent was added to a sample volume of 100 mL in a 125 mL Erlenmeyer flask; to avoid losing ammonia gas, the ammonia electrode inserted in a plastic gas-stopper was secured tightly on the top of the flask. Standards of 0.03-, 0.1- and 1 mg/L NH_3 as N were prepared daily to calibrate the probe. The ammonia standards and samples were then mixed vigorously with pH adjusting reagent using magnetic bar 10 minutes prior to recording the results.

Anions and cations in the filtered LW and WW2 samples were measured by ion chromatography (IC) using a Metrohm 850 IC with conductivity and UV detectors. The mobile phase was supplied by two eluent solutions – a sodium bicarbonate (3.6 mM) and an oxalic acid (3.5 mM). Stock standard solutions, supplied by Metrohm, were used to prepare separate anion and cation standard curves by dilution with Milli-Q water at concentrations of: 0.1-, 0.2-, 0.4-, 1.0-, and 10.0 mg L^{-1} (for cation) and 0.1-, 0.2-, 0.5-, 1-,

and 5 mg L^{-1} (for anion). The conditions for the cation method were as follows: Metrosep C4–150/4.0 column, flow of 0.900 mL min^{-1}, pressure of 5.07 MPa, temperature of 45°C and an elution time of 10 min. The conditions of the anion for conductivity-method were as follows: Metrosep A Supp 7–250/4.0 column, flow of 0.700 mL min^{-1}, pressure of 9.52 MPa, a temperature of 45°C and an elution time of 38 min. The conditions of the anion UV-detector method, which was to detect low-concentration species as Nitrite-N, Nitrate-N and Bromide, were similar as of the conductivity method, except having an elution time of 35 min.

2.5 Experimental procedures

Prior to beginning each DBPFP experiment, the source water was warmed to room temperature and amended with a 20 mM bicarbonate/carbonate buffer (Cimetiere et al., 2010) and adjusted to either pH of 7.0 or 8.3 using 1 N HCl or 1 N NaOH solution. Phosphate buffer was not used in this study because preliminary experiments showed this buffer caused precipitation in WW1 samples, likely caused by reactions between phosphate species and metals in the water. Additionally, phosphate ions are known to catalyze the auto-decomposition of NH_2Cl (Valentine and Jafvert, 1988).

For each source water (WW1, LW, and WW2), 30 sample waters were prepared for the DBP formation experiments, 10 samples for each of the three disinfection regimes. The FC7 experiments were designed to assess the effect of a 7-day free chlorine residual on THM4 and HAN formation following Standard Methods 5710-B (Eaton, 2005). Filtered source water was adjusted to pH 7.0 and chlorinated at doses from 4- to 120 mg L^{-1} as Cl_2 (Table 2) using a 5000 mg L^{-1} sodium hypochlorite stock solution standardized by Iodometric Method I (Eaton, 2005).

The MC7 and MC8 experiments were designed to study the effect of a 7-day monochloramine residual on THM4 and HAN formation. Filtered source waters were adjusted to pH 7.0 or 8.3 prior to being dosed with a preformed monochloramine solution at doses between 6 and 680 mg/L as Cl_2 (Table 2). To minimize the dilution error, the concentration of the monochloramine stock solution was of sufficient yield so that the maximum dosing volume was less than 5% of the sample volume. The preformed monochloramine solution was freshly prepared before the experiment by slowly dropping sodium hypochlorite solution into a rapidly mixing ammonium chloride solution (buffered at 20 mM $NaHCO_3$ and

adjusted to pH 8.3) to achieve a Cl_2:N mass ratio of 4.55:1. After 10 min of mixing, total chlorine, monochloramine, and total ammonia were measured. The monochloramine concentrations were measured using chloramine powder pillows (Method 10200 - Hach Company) on a spectrophotometer (Shimadzu UV-Vis 2450) at a wavelength of 655 nm, calibrated with a standard curve between 0.045 and 4.5 mg/L as Cl_2. Similarly, the total chlorine residuals were measured using DPD total chlorine total chlorine reagent powder pillows (Hach Company) at a wavelength of 552 nm, calibrated with a standard curve prepared in 250 mL amber bottles with doses between 1.0 and 5.0 mg/L as Cl_2. Measureable total ammonia residuals were purposfully achieved in the monochloramine solutions to minimize the concentration of unreacted free chlorine. To make higher concentrations of stock monochloramine for the experiments with WW2, the free chlorine and ammonia solutions were kept cold in a freezer for about 10 minutes prior to use and the ammonia solutions were then kept cold in an ice bath during mixing.

All dosed samples were kept headspace-free in 250-mL amber bottles capped with PTFE-lined lids, shielded from light at room temperature (25 ± 2^0C) for 7 days prior to measuring DBPs. To measure DBPs, a 400 mg quenching mix was added to 30 mL of sample water to stop THM formation reactions and slow HAN hydrolysis due to base-catalyzed degradation by decreasing pH to 4.5-5.5 using phosphate buffer. For the WW1 samples, the quenching mix used had a weight ratio of 9:1:39 (9 g ascorbic acid, 1 g KH_2PO_4, and 39 g Na_2HPO_4), which was confirmed to quench a 100 mg/L as Cl_2 free chlorine solution in preliminary experiments; for the WW2 samples, the quenching mix had a weight ratio of 18:1:39 due to higher doses of chlorine in these samples. After quenching, samples were extracted immediately by liquid/liquid extraction following EPA 551.1 with modifications as detailed in Pifer (2012). The remaining chlorinated samples were not chlorine quenched (for preservation) because the results showed that quenched samples had inconsistent DOC measurements. The remaining chlorinated samples were measured for pH, total ammonia, DOC, total chlorine and monochloramine residuals, UVA spectra (at 225 to 600 nm), and fluorescence EEMs within the next 24 hours.

2.6 Calculations for bromine-substituted THMs

To help assess THM speciation, the bromine substitution factor (BSF) and the total bromine incorporated (TotDXBr) were calculated following the work of others (Hua et al., 2006; Chow et al., 2007;

Hua and Reckhow, 2007; Engelage et al., 2009) using the following equations (with all DBP concentrations in mol L^{-1}):

$$BSF = \frac{(DCBM + 2 \times DBCM + 3 \times TBM)}{3 \times (TCM + DCBM + DBCM + TBM)}$$

$$TotDXBr = DCBM + 2 \times DBCM$$

3. Results and Discussion

3.1 Raw Water Quality Parameters

Raw water quality parameters for the three source waters are shown in Table 1. The pH of the three source waters was between pH 7.9-9.0 and the total ammonia ranged from 0.12-0.20 mg L^{-1} as N. The DOC of the wastewater sources (11.4- and 12.2 mg L^{-1} as C for WW1 and WW2, respectively) was greater than that of Beaver Lake (3.0 mg L^{-1} as C for LW), but the $SUVA_{254}$ values were similar (1.39-1.54 L mg^{-1} m^{-1}). This indicates the DOC of the three source waters had similar fractions of aromatic carbon. This is noteworthy because Weishaar et al. (2003) showed the total aromatic carbon content was proportional to THM formation following chlorination. Therefore, based on raw water DOC values, THM formation following chlorination of WW1 and WW2 should be higher than that of the LW.

Anions and cations were measured for LW and WW2 only. As expected, the concentrations of the five cations and seven anions were higher in WW2 compared to the LW. In terms of ions that impact DBP speciation, bromide ion was not detected in the LW and present at low concentrations (< 0.24 mg L^{-1}) in WW2, and thus chlorinated DBPs are expected to be the predominant species formed following chlorination and chloramination.

Sample waters were prepared from the three source waters by adjusting the pH followed by dosing with either free chlorine or monochloramine. Table 2 shows the pH of each sample at Days 0 and 7 and their corresponding doses of total ammonia, total chlorine, and monochloramine and these parameters and DOC and DIC measured on Day 7. For each of the three source waters (WW1, LW, and WW2), three sets of 10 samples were prepared, dosed with: (1) free chlorine at pH 7.0 (FC7), (2) monochloramine at pH 7.0 (MC7), and (3) monochloramine at pH 8.3 (MC8). As such, a total of nine

sample sets were produced (*Sample Sets 1-9*, Table 2), each consisting of 10 sample waters (90 total samples).

The FC7 experiment with WW1 was the first sample set produced and showed the greatest pH drift between Day 0 and Day 7. The pH of three of these samples increased by 0.6-0.8 log units (for FC doses of 6-, 30-, and 60 mg L^{-1} as Cl_2) but was measured after approximately 24 hours in a refrigerator at 4°C without first allowing the samples to warm to room temperature. For *Sample Sets 2-9*, the refrigeration step was bypassed and pH drift was typically less than 0.3 log units, demonstrating good pH buffering throughout the 7-day chlorination and chloramination periods, with the exception of MC8 samples at high monochloramine doses (>150 mg L^{-1} as Cl_2, *Sample Sets 6 and 9*) that dropped in pH between 0.4-0.7 log units. The control of pH is an important aspect of DBP formation experiments, as many DBPs are either general acid- or base-catalyzed. As such, in this study, caution must be exercised when drawing inferences from *Sample Set 1*.

The total ammonia was not measured for the FC7 samples (*Samples Sets 1, 4, and 7*, Table 2) and was present in the source waters at concentrations below 0.20 mg L^{-1} as N (Table 1). For MC7 and MC8, the total ammonia produced ("*Day 7*" minus "*Day 0*", Table 2) increased linearly with monochloramine demand ("*Dose*" minus "*Day 7*", Table 2), in agreement with previous research (Fairey et al., 2007). For MC7, least squares linear regression of these two parameters yielded regression coefficients, R^2, of 0.95 (for WW1), 0.95 (for LW), and 0.97 (for WW2) for *Samples Sets 2, 5, and 8*, respectively. Similarly, for MC8, the R^2 values were 0.98 (for WW1), 0.93 (for LW), and 0.98 (for WW2) for *Samples Sets 3, 6, and 9*, respectively. For each of the three source waters, the maximum monochloramine demand was higher at pH 7 than at pH 8.3 (Table 2 – 54.9- vs. 42.9 mg L^{-1} as Cl_2 for WW1, 485.6- vs. 143.9 mg L^{-1} as Cl_2 for LW, and 667.8- vs. 236.3 mg L^{-1} as Cl_2 for WW2). As such, DBP formation is expected to be higher for samples chloraminated at pH 7 compared to pH 8.3, in particular for species that are generally acid catalyzed.

Free chlorine doses ranged from 4-120 mg L^{-1} as Cl_2 were measured as total chlorine (Table 2). The total chlorine demand increased with free chlorine dose, but varied by source water type. For the two-wastewater effluents, the total chlorine demand varied from 5.9-29.5 mg L^{-1} as Cl_2 (*Sample Set 1*)

and 7.7-46.4 mg L^{-1} as Cl_2 (*Sample Set 7*). These demands were high compared to that of Beaver Lake, which varied from 2.5-7.4 mg L^{-1} as Cl_2 (*Sample Set 4*), despite a free chlorine dose as high as 80 mg L^{-1} as Cl_2. Taken together, these results reflect the high DOC in the wastewater sources compared to Beaver Lake (Table 1), and further suggest that DBP formation following chlorination should be higher in samples generated from the wastewater sources.

DOC and Dissolve Inorganic Carbon (DIC) were measured for *Sample Sets 1, 7, 8, and 9* in addition to a handful of other samples (Table 2). For the two FC7 groups measured (*Sample Sets 1 and 7)*, the DOC decreased with increasing applied free chlorine dose, with linear regression R^2 values of 0.79 and 0.68, respectively (data not shown), a trend found in previous research (Kozyatnyk et al., 2013). DOC decreased from 17.50- to 13.22 mg L^{-1} as C for *Sample Set 1* (WW1, pH 7.0) and from 17.90- to 5.68 mg L^{-1} as C for *Sample Set 7* (WW2, pH 7.0), although the extent of decrease was similar for a given free chlorine dose (e.g., for 60 mg L^{-1} as Cl_2, Table 2). These decreases in DOC were not offset by concomitant increases in DIC (Table 2), indicating volatilization of inorganic carbon species likely occurred. Similarly, for the two MC groups measured (*Sample Sets 8 and 9*), DOC decreased with increasing applied monochloramine dose, with linear regression R^2 values of 0.94 and 0.71, respectively. DOC decreased from 15.10- to 13.00 mg L^{-1} as C for *Sample Set 8* (WW2, pH 7) and from 17.00- to 16.20 mg L^{-1} as C for *Sample Set 9* (WW2, pH 8.3), losses which again were not offset by increases in DIC. The greater decrease in DOC at pH 7.0 compared to pH 8.3, is in agreement with the higher monochloramine demand at the lower pH (Table 2).

3.2 Formation of THMs

3.2.1 TCM

Fig. 1a shows the formation of TCM as a function of chlorine residual (CR) after a 7-day free chlorination period for the three sources waters (WW1, LW, and WW2). The TCM concentrations increased, following the pattern of a typical exponential recovery curve, through the highest CR evaluated (~75 mg L^{-1} as Cl_2 for LW and WW2), and indicated the maximum TCMFP was not reached. Given the chlorine dose and CR followed a similar pattern (Table 2, *Sample Sets 1, 4,* and *7*), the results shown in Fig. 1a are in agreement with previous research (Nikolaou et al., 2004; Sun et al., 2013) that presented

TCM formation as a function of chlorine dose as opposed to CR. The large successive increases in TCM formation at low CR (i.e. < 20 mg L^{-1} as Cl_2) may have been due to increased chlorine availability (as CR increases) in the reaction between chlorine and dissolved organic carbon (DOC). However, the near linear increase of TCM at high CR (i.e., > 20 mg L^{-1} as Cl_2) may indicate a decrease of DOC availability (Table 2) for these same reactions. Stated another way, TCM formation was chlorine-limited at low CR and DOC-limited at high CR. At a CR between 3-5 mg L^{-1} as Cl_2 – the recommended residual for THMFP in Standard Methods 5710 B (Eaton, 2005) – the TCM concentrations of the three source waters were approximately 60-70% of their maximum values relative to the highest CRs achieved (30.5-, 72.6-, and 73.6 mg L^{-1} as Cl_2 for WW1, LW, and WW2, respectively). However, based on the trends shown in Fig. 1a, the TCM concentrations would likely continue to increase at even higher values of CR, and thus the 60-70% is an overestimate. It is noteworthy that WW1 and WW2 had similar TCM concentrations at CR ~1 mg L^{-1} as Cl_2 (~230 µg L^{-1}) but dissimilar TCM concentrations at CR 3-5 mg L^{-1} as Cl_2 (273- and 385- µg L^{-1} for WW1 and WW2, respectively). This result indicates the arbitrary nature of using a given value of CR for comparing TCM formation between different water sources. Further, although the three source waters had similar TCM profiles, there were strong linear correlations between TCM and chlorine demand of WW1 and WW2 (R^2 > 0.98) but not LW (R^2 = 0.48). This suggests the lake water may contain more reduced inorganics (e.g., iron (II)) that exerted a chlorine demand but did not react to form TCM and/or the nature of THM precursors in the WWs and LW were different, a contention supported by previous research (Sirivedhin and Gray, 2005).

Fig. 1b shows TCM as a function of CR after a 7-day chloramination period for the three source waters at pH 7.0 and 8.3. For MC8, TCM of the LW and WW2 increased with CR and leveled off at a CR of ~30 mg L^{-1} as Cl_2. The TCM profile of WW1 overlaid with that of WW2 (inset of Fig. 1b), despite the former having a maximum CR of only 17.1 mg L^{-1} as Cl_2 (Table 2, *Sample Set 3*). At a CR of 3-5 mg L^{-1} as Cl_2 – the recommended residual for DBPFP in Standard Methods 5710 B (Eaton, 2005) – the TCM concentrations were ~30% and 25% their maximums achieved at high CR (~30 mg L^{-1} as Cl_2) for LW and WW2, respectively. It was unexpected that the TCM profiles for the two WWs were similar for MC8 (~10 µg L^{-1} at CR 3-5 mg L^{-1} as Cl_2, inset of Fig. 1b) but different for FC (273- and 385 µg L^{-1} for WW1 and WW2, respectively, at CR 3-5 mg L^{-1} as Cl_2, Fig. 1a) This result suggests that the variability in TCM

formation between source waters increases with the reactivity of the disinfectant applied (e.g., with FC more reactive than MC).

In the MC7 experiment (inset of Fig. 1b), TCM of the three source waters increased with CR, following a typical exponential recovery curve. For all values of CR, TCM of the three waters was higher for MC7 than MC8, indicating TCM formation was general acid catalyzed during chloramination, which is in agreement with the findings of Cimetiere et al. (2010). Interestingly, TCM formation has been shown to be general base catalyzed during chlorination (Hua and Reckhow, 2008), a result that could not be verified by this study given that free chlorine was assessed at pH 7 only. The higher TCM concentration for MC7 relative to MC8 may be in part due to: (1) an increase of monochloramine hydrolysis at lower pH (Diehl et al., 2000), which increases the ratio of FC in equilibrium with MC thereby enhancing DBP formation (Zhang et al., 1999); (2) the presence of dichloramine, an undesired species present during chloramination in equilibrium with monochloramine, which is favored at lower pH (Jafvert and Valentine, 1992) and may play an important role in DBP formation (Yang et al., 2007) and (3) higher monochloramine doses for MC7 than MC8 to achieve a given CR (Table 2) to compensate for faster monochloramine autodecomposition (Diehl et al., 2000).

3.2.2 DCBM

Fig. 1c shows the formation of DCBM as a function of CR after a 7-day free chlorination period for the three source waters. The DCBM concentrations of the two WWs increased with CR to ~4 mg L^{-1} as Cl_2 and leveled off thereafter, while the DCBM of the LW decreased at CR values in excess of ~40 mg L^{-1} as Cl_2. DCBM profiles in chlorinated WW1 and WW2 were similar at low CR (< 1 mg L^{-1} as Cl_2) but deviated from one another at CR in excess of 3 mg L^{-1} as Cl_2 (116.4- and 94 µg L^{-1} for WW1 and WW2, respectively, at CR 3-5 mg L^{-1} as Cl_2). Between these residuals, the DCBM concentrations were ~90-95% their maximum values, which occurred at a CR of ~20 mg L^{-1} as Cl_2 for the two WWs, indicating the true formation potential was achieved. When compared to TCM (Fig. 1a), this result suggests that bromide ion availability limited DCBM formation at high CR, and was fully incorporated as bromine at relatively low CR values (~5 mg L^{-1} as Cl_2). This result may be explained by known reaction pathways (e.g., oxidation and

incorporation) between free chlorine and NOM in the presence of bromide, as summarized by Hua et al. (2006):

(1) $HOCl + Br^- \rightarrow HOBr + Cl^-$ $k_1 = 1{,}550\ M^{-1}\ s^{-1}$ (Kumar and Margerum, 1987)

(2) $HOCl + NOM \rightarrow Products$ $k_2 = 0.7\text{-}5\ M^{-1}\ s^{-1}$ (Westerhoff et al., 2004)

(3) $HOBr + NOM \rightarrow Products$ $k_3 = 15\text{-}167\ M^{-1}\ s^{-1}$ (Westerhoff et al., 2004)

Based on the kinetics of these reactions, brominated DBPs – produced through reaction (3) are likely limited by hypobromous acid concentration which itself is produced by the oxidation of bromide in reaction (1), even at low free chlorine concentrations.

Fig. 1d shows the formation of DCBM as a function of CR after a 7-day chloramination period for the three source waters at pH 7 and 8.3. In the MC8 experiment, the DCBM formation increased linearly with CR for all waters (R^2 = 0.97, 0.95. and 0.99, for WW1, LW, and WW2, respectively), although DCBM concentrations were relatively small compared to their maximum values between 3-5 mg L^{-1} as Cl_2 CR (2.7-, 0.2-, and 0.9 µg L^{-1} for WW1, LW, and WW2, respectively). In the MC7 experiment, DCBM concentrations increased, following a typical exponential recovery curve, although at CR values greater than ~10 (which corresponded to monochloramine doses larger 200- and 350 mg L^{-1} as Cl_2 for LW and WW2 – Table 2), DCBM decreased sharply, which could not be explained based on the data collected in this study. At CR 3-5 mg L^{-1} as Cl_2 – the recommended residual for DBPFP in Standard Methods 5710 B (Eaton, 2005) – DCBM concentrations of WW1, LW, and WW2 were ~31.5-, 4.7-, 35.2 µg L^{-1}, respectively which represented ~96-, 95-, and 76% of its maximum values (achieved at CR of 17.4-, 9.1, and 13.7 mg L^{-1} as Cl_2), respectively. It should be noted that, similar to TCMFP, the relative differences between DCBM concentrations of WW1 and WW2 increased with the reactivity of the disinfectants (i.e., FC > MC7 > MC8).

3.2.3 DBCM

Fig. 1e shows DBCM as a function of CR after a 7-day free chlorination period for the three source waters. DBCM concentrations varied with CR but showed similar trends for each source water, with maximum formation potentials between 40-42 µg L^{-1} for the two WWs and 3 µg L^{-1} for the LW. The

DBCM concentrations peaked at a CR of approximately 1 mg L^{-1} as Cl_2 and decreased thereafter through the highest CR evaluated (~75 mg L^{-1} as Cl_2). At CR 3-5 mg L^{-1} as Cl_2, DBCM concentrations for WW1, LW, and WW2 were ~31.3-, 2.1-, and 33.9 μg L^{-1}, respectively, which comprised approximately 70-80% its maximum values.

Fig. 1f shows DBCM as a function of CR after a 7-day chloramination period for the three source waters at pH 7.0 and 8.3. In MC8 experiment, DBCM in LW formed at concentrations below than the lowest GC standard (1 μg L^{-1}), and hence is not discussed. DBCM in the two WWs generally increased linearly with CR, with an exponential increase in WW2 at a CR in excess of 60 mg L^{-1} as Cl_2. At CR between 3-5 mg L^{-1} as Cl_2, DBCM of WW1 and WW2 was ~1- and 0.4 μg L^{-1} which comprised ~30% and 3%, respectively, its values at the highest CRs evaluated (17.1- and 63.7 mg L^{-1} as Cl_2 for WW1 and WW2, respectively). For MC7, DBCM peaked at CR of ~2.5 mg L^{-1} as Cl_2 for WW1 and LW and ~4 mg L^{-1} as Cl_2 for WW2 (19.8-, 1.2-, and 17.3 μg L^{-1} for WW1, LW, and WW2, respectively). These peaks were followed by decreases in DBCM as CR increased, resulting in DBCM values at CR 3-5 mg L^{-1} as Cl_2 of approximately 90% of their maximum values for WW1 and LW. It is also noteworthy that the differences in DBCMFP between the WWs and LW were approximately 15 times in both the FC7 and MC7 experiments. Further, DBCMFP for the LW was below the GC detection limits in MC8 experiment, indicating that the bromide ion was low in the LW (Table 1) and more readily oxidized into DBCM with free chlorine compared to monochloramine in the WWs.

3.2.4 TBM

Fig. 1g shows the formation of TBM as a function of CR after a 7-day free chlorination period for the two WWs only (TBM of the LW formed at concentrations below the detection limit of 1 μg L^{-1} and was not shown). TBM concentrations of the two WWs peaked (at 2-, and 2.6 μg L^{-1} for WW1 and WW2, respectively) at CR ~1.5 mg L^{-1} as Cl_2 and decreased thereafter with increasing CR. At CR 3-5 mg L^{-1} as Cl_2, TBM concentration of WW1 and WW2 were 80- and 90% its maximum values, respectively.

Fig. 1h shows the formation of TBM as a function of CR after a 7-day chloramination period for the two WWs at pH 7 and 8.3 (TBM of the LW formed at concentrations below the detection limit of 1 μg L^{-1} and were not shown). For MC8, TBM only formed above this threshold at a CR in excess of 60 mg L^{-1}

as Cl_2 and is therefore not discussed. For MC7, TBM of the two WWs peaked at concentrations less than 2 μg L^{-1}, at CRs of ~1.5-, and 4 mg L^{-1} Cl_2 for WW1 and WW2, respectively and decreased with increasing CR. TBM of WW1 at CR 3-5 mg L^{-1} as Cl_2 was ~35-65% of its maximum concentration.

All bromine-substituted THMs formed at higher concentrations in the MC7 experiments compared to the MC8 experiments (Fig. 1d, f, h). As suggested by previous research (Le Roux et al., 2012), this may be attributed to the presence of HOBr produced by monochloramine autodecomposition into free chlorine, a reaction that is favored at lower pH. However, the decrease of DBCM and TBM at CR values in excess of ~1-3 mg L^{-1} as Cl_2 in the FC7 and MC7 experiments suggests that the formation of these species decreases with the increase of free chlorine residual and ammonia concentrations present in sample waters.

3.3 Formation of HANs

3.3.1 DCAN

Fig. 2a shows DCAN as a function of CR after a 7-day free chlorination period for the three source waters. DCAN concentrations varied with CR but showed similar trends among the source waters, with maximum formation potentials between 24-26 μg L^{-1} for the two WWs and 4 μg L^{-1} for the LW. The DCAN concentrations peaked at a CR of approximately 1.5 mg L^{-1} as Cl_2 and decreased exponentially thereafter and asymptotically approached zero at a CR of ~20 mg L^{-1} as Cl_2. This pattern of DCAN formation is consistent with previous research (Reckhow et al., 2001; Sun et al., 2013) that showed hydrolysis of DCAN was catalyzed by hypochlorite ion. At a CR between 3-5 mg L^{-1} as Cl_2, the DCAN concentration was only 35-65% of its maximum values and decreased throughout this target window (inset of Fig. 2a). The true maximum DCANFP occurred at a CR of 1.5 mg L^{-1} as Cl_2, which is especially relevant because this is close to the target residual present in many drinking water distribution systems that use free chlorine.

Fig. 2b shows DCAN formation for the three source waters as a function of CR after a 7-day chloramination period at pH 7.0 and 8.3. In the MC8 experiment, the DCAN formation increased with the increasing CR for all waters (R^2 = 0.87, 0.97, and 0.99 for WW1, LW, and WW2, respectively). A linear

relationship was also present between DCAN and chloramine dose (Table 2) with R^2 = 0.94, 0.99, and 0.97 for WW1, LW, and WW2, respectively. This result is in agreement with the findings in Yang (2007), that showed a linear relationship between DCAN and chloramine dose (R^2 = 0.98), although these experiments were conducted at pH 7.5 using a 3-day chloramination period. However, for the MC8 experiments, it is noteworthy that DCAN concentrations were small (< 1 μg L^{-1}) between 3-5 mg L^{-1} as Cl_2 CR.

In the MC7 experiment (Fig. 2b), the DCAN-CR relationship for the LW was linear (R^2 = 0.98), however the pattern for the two WWs followed an exponential recovery curve (R^2 = 0.99 and 0.94, for WW1 and WW2, respectively). At a CR between 3-5 mg L^{-1} as Cl_2, the DCAN concentrations were approximately 9.5-, 1.6-, and 28.6 μg L^{-1} for WW1, LW, and WW2 respectively. Although DCAN formation has been shown to be dependent on the presence of specific compounds and reactions between organic-N compounds and chloramines (Chen, 2011; Yang et al., 2012), the results in this study agree with the general trend of decreasing DCAN formation with increasing pH of chloramination between pH 7 and 9 (Yang et al., 2007). This result may be in part due to the based-catalyzed decomposition of DCAN (Reckhow et al., 2001) and the higher doses of MC7 relative to MC8 (to achieve a given CR, Table 2). The higher DCAN formation in the wastewaters compared to the lake water (by approximately a factor of 10) indicates these precursors were enriched in the wastewater effluent samples.

It should be noted that there were significant differences in DCAN concentrations between the two wastewaters in the MC7 experiment (9.5 μg L^{-1} for WW1 and 28.6 μg L^{-1} for WW2 at CR 3-5 mg L^{-1} as Cl_2). This was unexpected because the DCAN concentrations in the FC experiment (Fig. 2a) were similar in the two WWs at all CRs (12.7 μg L^{-1} for WW1 and 9.8 μg/L for WW2 at CR 3-5 mg L^{-1} as Cl_2). These seemingly conflicting results may illuminate the two major HAN formation pathways, which are: (1) the decarboxylation pathway where FC or MC reacts with free amino acids, and (2) the aldehyde pathway where MC nitrogen is incorporated into an aldehyde (Shah and Mitch, 2011). Thus, in this study, the two WWs may have had comparable concentrations of free amino acids leading to similar DCAN formation during free chlorination, but WW2 had a greater abundance of aldehydes, leading to enhanced DCAN formation during chloramination. This result implies that the relative differences in DCANFP between

source waters are dependent on the disinfectant type (e.g. FC or MC). It is also noteworthy that for WW2, DCAN concentrations for MC7 were higher than for FC7 between a CR 3-5 mg L^{-1} as Cl_2, which is opposite of previously reported findings (Hua and Reckhow, 2007; Dotson et al., 2009; Bougeard et al., 2010; Fang et al., 2010) that compared DCANFP of samples with the same dose of FC or MC.

3.3.2 DBAN

Fig. 2c shows DBAN formation as a function of CR after a 7-day chlorination period for the two WWs (DBAN formation in the lake water was below the detection limit of 1 µg L^{-1}). Similar to the DCAN formation trend shown in Fig. 2a, DBAN concentrations varied with CR but had a similar pattern for the two WWs. The maximum DBAN concentrations of 4.5 µg L^{-1} for WW1 and 1.6 µg/L for WW2 occurred at a CR of approximately 1 mg L^{-1} as Cl_2 for both waters, and then decreased thereafter and asymptotically approached zero at a CR of ~20 mg L^{-1} as Cl_2. At a CR between 3-5 mg L^{-1} as Cl_2, the DBAN concentration was about 4.5- and 1.6 µg L^{-1} for WW1 and WW2, respectively, which is only 50-70% their maximum values. Although DCAN and DBAN formation profiles for chlorination were similar, there was a difference in the CR values at the maximum FP for the two compounds (i.e. 1.0- and 1.5 mg L^{-1} as Cl_2 for DBAN and DCAN, respectively) that cannot be explained based on the data collected in this study.

Fig. 2d shows DBAN formation as a function of CR after a 7-day chloramination period for the two WWs at pH 7.0 and 8.3. DBAN concentrations in the lake water and MC8 experiment were below the detection limit of 1 µg L^{-1} and are not discussed further. For MC7, DBAN peaked at CR of ~1 mg L^{-1} as Cl_2 (at concentrations of 3.1 µg/L for WW1 and 1.0 µg L^{-1} for WW2) and then decreased as CR increased, resulting in DBAN values at a CR 3-5 mg L^{-1} as Cl_2 of approximately 40-55% for WW1 and 75% for WW2 of their maximum values.

3.4 Summary of DBPFP experiments

Table 3 shows a summary of the values of CR corresponding to the maximum concentrations of each DBP in the formation potential experiments, termed CR_{MAX}. There were differences in CR_{MAX} between the three disinfection regimes (e.g., FC7, MC7, and MC8) for all DBPs except DBAN, illustrating the true formation potential was dependent on the disinfectant type and pH. In comparison to the SM5710 B (for THMs) and SM5710 D (for HANs), no DBPs were maximized between the 3-5 mg L^{-1} as Cl_2 target

window, suggesting other CR values (i.e., Table 3) would be more appropriate to assess DBP-precursor removal processes. It is important to note that the CR_{MAX} values for the bromine-substituted THMs is a function of the low bromide concentrations present in the source waters used in this study (Table 1) and would likely be higher for bromide-rich samples. The DCAN results (Fig. 2a and 2b and Table 3) indicate that assessment of precursor removal processes for this DBP is likely most accurately assessed under chloramination conditions at pH 7.0.

3.5 Bromine-substituted THM speciation

Fig. 3 shows the DCBM and DBCM concentrations (in μmol bromine L^{-1}), the sum total of these species (TotDXBr), and the THM bromine substitution factor (BSF) as a function of CR after the 7-day free chlorination period at pH 7 for WW1 (Fig. 3a), LW (Fig. 3b), and WW2 (Fig. 3c). TBM was ignored in these calculations because it was formed at such low concentrations (less than 3 μg L^{-1}, Fig. 2) throughout these experiments. For all source waters, the concentration of DCBM was higher than DBCM, an expected result given the stepwise bromine-substitution pattern for THMs. The TotDXBr of the two WWs peaked at a concentration of ~1 μmol bromine L^{-1}, which corresponded to a CR ~1.2-1.5 mg L^{-1} as Cl_2, and was relatively constant thereafter. This profile was similar for LW, but the TotDXBr values were smaller by about an order of magnitude presumably because of the lower bromide concentration (Table 1). These results suggest that bromime was fully incorporated into DCBM and DBCM at relatively low values of CR (< 5 mg L^{-1} as Cl_2), in agreement with the findings of Chang (2001). Further, the general trend of decreasing BSF with the increasing of FC dose (Fig. 3) is in agreement with findings of Hua (2012), and reflect the bromide ion limitation coupled with the increased TCM formation with CR (Fig. 2a).

Fig. 4 shows the DCBM and DBCM concentrations (in μmol bromine L^{-1}), the sum total of these species (TotDXBr), and the THM BSF as a function of CR after the 7-day chloramination period at pH 7.0 (MC7) and 8.3 (MC8) for the three source waters. The TotDXBr values for the LW experiments were less than 0.05 (Fig. 4b and 4e), indicating the fraction of bromine-substituted species was low throughout and therefore are not discussed further. For a given chloramination pH (7.0 or 8.3), the bromine substitution patterns were similar for WW1 (Fig. 4a and 4d) and WW2 (Fig. 4c and 4f), although the concentration of these species were approximately a factor of two larger at pH 7.0. For MC7, DCBM, DBCM, and TotDXBr

increased following a typical exponential recovery curve and leveled off at CR values in excess of ~5- and 3 mg L^{-1} as Cl_2 for WW1 and WW2, respectively. BSF generally decreased with CR, similar to the pattern with FC (Fig. 3), indicating bromide ion limited the formation of bromine-substituted THMs. In contrast, for MC8, all parameters in Fig. 4d and 4f increased with CR, indicating the rate of bromide oxidation was limiting, as opposed to bromide ion itself. These results are in agreement with findings Hua (2008) that showed the increased reactivity of monochloramine at lower pH led to increased formation of chlorine- and bromine-substituted THMs.

3.6 Precursor surrogate parameters for TCM and DCAN

TCM, the predominant THM formed in the chlorination and chloramination experiments (Fig. 2), was regressed against each measured fluorescence excitation-emission wavelength pair, $I_{Ex/Em}$, for the WW1 and WW2 samples (Table 2, *Samples Sets 1-3* for WW1 and *7-9* for WW2). Fluorescence EEMs were not collected for the LW samples because of a scheduling conflict that occupied the instrument. Fig. 5 shows the R^2 values from the TCM-$I_{Ex/Em}$ regressions for FC7 (Fig. 5a and 5d), MC7 (Fig. 5b and 5e) and MC8 (Fig. 5c and 5f). For FC7, there were strong correlations between TCM and $I_{Ex/Em}$ across large portions of the EEMs, with $R^2 > 0.95$ between excitation wavelengths of ~225-350 nm and emission wavelengths of ~375-500 nm. A similarly strong set of correlations were also found for DCBM (data not shown). As such, $I_{Ex/Em}$ data were strong TCM (and DCBM) precursor surrogate parameters for the WW samples dosed with free chlorine between 4-120 mg L^{-1} as Cl_2. In contrast, for MC7, the R^2 were less than 0.4 throughout both EEMs (Fig. 5b and 5e), indicating fluorescence $I_{Ex/Em}$ values were not good TCM precursor surrogate parameters for chloramination at pH 7. Similarly weak correlations were found for MC8 (Fig. 5c and 5f).

Fig. 6 was formulated in a similar manner as Fig. 5, only that DCAN was regressed against the $I_{Ex/Em}$ values, instead of TCM. However, the R^2 values less than 0.6 throughout for FC7, MC7, or MC8, indicating that fluorescence $I_{Ex/Em}$ values were not useful DCAN precursor surrogate parameters.

Fig. 7 shows the R^2 values between (i) TCM and UVA and (ii) DCAN and UVA for the two WWs (60 total samples) in the FC7 (Fig. 7a and 7d), MC7 (Fig. 7b and 7e), and MC8 (Fig. 7c and 7f) experiments. For TCM, R^2 values for WW1 (Fig. 7a) were greater than 0.8 between 235-255 nm, but less

than 0.5 in this same range for WW2 (Fig. 7b). As such, UV was not a consistently accurate THM precursor surrogate parameter for FC7. In contrast, TCM-UVA R^2 values for MC7 and MC8 were greater than 0.9 between 325-350 nm, indicating $UV_{325-350}$ was a strong THM precursor surrogate parameter for both wastewaters. For DCAN, R^2 values for FC7 were less than 0.4; while the R^2 values were high for MC7 and MC8 in discrete ranges, there were no UV values with R^2 values consistently above 0.8, suggesting UV was not a reliable DCAN precursor surrogate for chloramination.

4. Conclusions

The experiments presented here demonstrate that the DBPFP tests described in Standard Methods (Eaton, 2005) do not yield the true or, more precisely, the maximum DBPFP at the recommended CR of 3-5 mg L^{-1} as Cl_2. Rather, the data indicate that the DBPFP for a given compound (e.g. TCM or DCAN) occurred at a range of CR values (1.0 to >70 mg L^{-1} as Cl_2) and was dependent on the disinfectant type and pH of the sample water. The true DBPFP was not reached for some compounds (e.g., TCM for FC7 and MC7, most THMs and HANs for MC8) despite CR values in excess of 70 mg L^{-1} as Cl_2. While some bromine-substituted THMs appeared to reach maximum values near the recommended CR of 3-5 mg L^{-1} as Cl_2 (e.g., DBCM and TBM for MC7), a bromide ion limitation was likely responsible. For DCAN, the predominant HAN formed, the CR_{MAX} was 1.5-1.7 mg L^{-1} as Cl_2 for FC7 and in excess of 15 mg L^{-1} as Cl_2 for MC7 and MC8. The results of this study demonstrate the impact of CR on the formation of THMs and HANs, and can be leveraged to help assess various DBP-precursor removal processes and be used to guide development of more a more robust DBPFP test.

5. References

Bougeard, C. M. M., Goslan, E. H., Jefferson, B. and Parsons, S. A., 2010. Comparison of the disinfection by-product formation potential of treated waters exposed to chlorine and monochloramine. Water Research 44 (3), 729-740.

Chang, E. E., Lin, Y. P. and Chiang, P. C., 2001. Effects of bromide on the formation of THMs and HAAs. Chemosphere 43 (8), 1029-1034.

Chen, B. Y., 2011. Hydrolytic Stabilities of Halogenated Disinfection Byproducts: Review and Rate Constant Quantitative Structure-Property Relationship Analysis. Environmental Engineering Science 28 (6), 385-394.

Chow, A. T., Dahlgren, R. A. and Harrison, J. A., 2007. Watershed sources of disinfection byproduct precursors in the Sacramento and San Joaquin rivers, California. Environmental Science & Technology 41 (22), 7645-7652.

Cimetiere, N., Dossier-Berne, F. and De Laat, J., 2010. Effect of some parameters on the formation of chloroform during chloramination of aqueous solutions of resorcinol. Water Research 44 (15), 4497-4504.

Diehl, A. C., Speitel, G. E., Symons, J. M., Krasner, S. W., Hwang, S. J. and Barrett, S. E., 2000. DBP formation during chloramination. Journal American Water Works Association 92 (6), 76-90.

Dotson, A., Westerhoff, P. and Krasner, S. W., 2009. Nitrogen enriched dissolved organic matter (DOM) isolates and their affinity to form emerging disinfection by-products. Water Science and Technology 60 (1), 135-143.

Eaton, A. D., Clesceri, L.S., Rice, E.W., Greenberg, A.E. (Eds.) (2005). Standard Methods for the Examination of Water & Wastewater American Public Health Association, Washington, DC. .

Engelage, S. K., Stringfellow, W. T. and Letain, T., 2009. Disinfection Byproduct Formation Potentials of Wetlands, Agricultural Drains, and Rivers and the Effect of Biodegradation on Trihalomethane Precursors. Journal of Environmental Quality 38 (5), 1901-1908.

Fairey, J. L., Speitel, G. E. and Katz, L. E., 2007. Monochloramine destruction by GAC - effect of activated carbon type and source water characteristics. Journal American Water Works Association 99 (7), 110-120.

Fang, J. Y., Yang, X., Ma, J., Shang, C. and Zhao, Q. A., 2010. Characterization of algal organic matter and formation of DBPs from chlor(am)ination. Water Research 44 (20), 5897-5906.

Granderson, C. W., Pifer, A. D. and Fairey, J. L., 2013. An improved chloroform surrogate for ClO_2 and alum treated waters. Journal American Water Works Association 105 (3), E103-E114.

Hua, G. H. and Reckhow, D. A., 2007. Comparison of disinfection byproduct formation from chlorine and alternative disinfectants. Water Research 41 (8), 1667-1678.

Hua, G. H. and Reckhow, D. A., 2008. DBP formation during chlorination and chloramination: Effect of reaction time, pH, dosage, and temperature. Journal American Water Works Association 100 (8), 82-+.

Hua, G. H. and Reckhow, D. A., 2012. Evaluation of bromine substitution factors of DBPs during chlorination and chloramination. Water Research 46 (13), 4208-4216.

Hua, G. H., Reckhow, D. A. and Kim, J., 2006. Effect of bromide and iodide ions on the formation and speciation of disinfection byproducts during chlorination. Environmental Science & Technology 40 (9), 3050-3056.

Jafvert, C. T. and Valentine, R. L., 1992. Reaction Scheme for the Chlorination of Ammoniacal Water. Environmental Science and Technology 26 (3), 577.

Kozyatnyk, I., Swietlik, J., Raczyk-Stanislawiak, U., Dabrowska, A., Klymenko, N. and Nawrocki, J., 2013. Influence of oxidation on fulvic acids composition and biodegradability. Chemosphere 92 (10), 1335-1342.

Kumar, K. and Margerum, D. W., 1987. KINETICS AND MECHANISM OF GENERAL-ACID-ASSISTED OXIDATION OF BROMIDE BY HYPOCHLORITE AND HYPOCHLOROUS ACID. Inorganic Chemistry 26 (16), 2706-2711.

Le Roux, J., Gallard, H. and Croue, J. P., 2012. Formation of NDMA and Halogenated DBPs by Chloramination of Tertiary Amines: The Influence of Bromide Ion. Environmental Science & Technology 46 (3), 1581-1589.

Muellner, M. G., Wagner, E. D., McCalla, K., Richardson, S. D., Woo, Y. T. and Plewa, M. J., 2007. Haloacetonitriles vs. regulated haloacetic acids: Are nitrogen-containing DBPs more toxic? Environmental Science & Technology 41 (2), 645-651.

Nikolaou, A. D., Golfinopoulos, S. K., Lekkas, T. D. and Arhonditsis, G. B., 2004. Factors affecting the formation of organic by-products during water chlorination: A bench-scale study. Water Air and Soil Pollution 159 (1-4), 357-371.

Pifer, A. D. and Fairey, J. L., 2012. Improving on $SUVA_{254}$ using fluorescence-PARAFAC analysis and disinfection byproduct formation and control. Water Research 46 (9), 2927-2936.

Reckhow, D. A., Platt, T. L., MacNeill, A. L. and McClellan, J. N., 2001. Formation and degradation of dichloroacetonitrile in drinking waters. Journal of Water Supply Research and Technology-Aqua 50 (1), 1-13.

Rook, J. J., 1976. HALOFORMS IN DRINKING-WATER. Journal American Water Works Association 68 (3), 168-172.

Seidel, C. J., McGuire, M. J., Summers, R. S. and Via, S., 2005. Have utilities switched to chloramines? Journal American Water Works Association 97 (10), 87-97.

Shah, A. D. and Mitch, W. A. (2011). Halonitroalkanes, Halonitriles, Haloamides, and N-Nitrosamines:A Critical Review of Nitrogenous Disinfection Byproduct FormationPathways, American Chemical Society.

Sirivedhin, T. and Gray, K. A., 2005. 2. Comparison of the disinfection by-product formation potentials between a wastewater effluent and surface waters. Water Research 39 (6), 1025-1036.

Sun, X. B., Sun, L., Lu, Y. and Jiang, Y. F., 2013. Factors affecting formation of disinfection by-products during chlorination of Cyclops. Journal of Water Supply Research and Technology-Aqua 62 (3), 169-175.

Thermo-Scientific. "Thermo Scientific™ Orion HP Ammonia User Guide."

USEPA. (1999). "EPA Guidance Manual Alternative Disinfectants and Oxidants."

USEPA. (2006). "Stage 2 Disinfectants and Disinfection Byproducts Rule, 40 CFR, Parts 9, 141, and 142."

Valentine, R. L. and Jafvert, C. T., 1988. GENERAL ACID CATALYSIS OF MONOCHLORAMINE DISPROPORTIONATION. Environmental Science & Technology 22 (6), 691-696.

Weishaar, J. L., Aiken, G. R., Bergamaschi, B. A., Fram, M. S., Fujii, R. and Mopper, K., 2003. Evaluation of specific ultraviolet absorbance as an indicator of the chemical composition and reactivity of dissolved organic carbon. Environmental Science & Technology 37 (20), 4702-4708.

Westerhoff, P., Chao, P. and Mash, H., 2004. Reactivity of natural organic matter with aqueous chlorine and bromine. Water Research 38 (6), 1502-1513.

Yang, X., Shang, C. and Westerhoff, P., 2007. Factors affecting formation of haloacetonitriles, haloketones, chloropicrin and cyanogen halides during chloramination. Water Research 41 (6), 1193-1200.

Yang, X., Shen, Q. Q., Guo, W. H., Peng, J. F. and Liang, Y. M., 2012. Precursors and nitrogen origins of trichloronitromethane and dichloroacetonitrile during chlorination/chloramination. Chemosphere 88 (1), 25-32.

Zhang, X. R., Echigo, S., Minear, R. A. and Plewa, M. J., 1999. Characterization and comparison of disinfection by-products from using four major disinfectants. Abstracts of Papers of the American Chemical Society 217, U736-U736.

List of Tables

Parameter	Units	Noland Effluent WW1	Noland Effluent WW2	Beaver Lake LW
pH		8.3	7.9	9.0
DOC	mg L^{-1} as C	11.4	12.2	3.0
UVA_{254}	cm^{-1}	0.162	0.188	0.042
$SUVA_{254}$	L mg^{-1} m^{-1}	1.42	1.54	1.39
Total Ammonia	mg L^{-1} as N	0.12	0.20	0.12
Cations				
Lithium	mg L^{-1}	NM	0.03	ND
Sodium	mg L^{-1}	NM	87.04	3.48
Potassium	mg L^{-1}	NM	22.45	1.80
Calcium	mg L^{-1}	NM	4.29	2.18
Magnesium	mg L^{-1}	NM	46.39	22.25
Anions				
Fluoride	mg L^{-1}	NM	0.59	0.09
Chloride	mg L^{-1}	NM	77.22	3.58
Nitrite-N	mg L^{-1}	NM	0.23	ND
Nitrate-N	mg L^{-1}	NM	35.42	0.15
Bromide	mg L^{-1}	NM	0.24	ND
Phosphate	mg L^{-1}	NM	1.13	ND
Sulfate	mg L^{-1}	NM	58.87	8.19

WW1 – wastewater effluent collected on 7/24/13; WW2 – wastewater effluent collected on 9/19/13; LW – lake water collected on 8/28/13; DOC: dissolved organic carbon; UVA_{254}: ultraviolet absorbance at 254 nm; $SUVA_{254}$: specific ultraviolet absorbance at 254 nm; NM: not measured; ND: not detected

Table 2. pH, total ammonia, total chlorine, monochloramine, and DOC of the sample waters

pH		Total Ammonia ($mg\ L^{-1}$ as N)		Total Chlorine ($mg\ L^{-1}$ as Cl_2)		Monochloramine ($mg\ L^{-1}$ as Cl_2)		DOC ($mg\ L^{-1}$ as C)	DIC ($mg\ L^{-1}$ as C)
Day 0	Day 7	Dose	Day 7	Dose	Day 7	Dose	Day 7	Day 7	Day 7
WW1 – Noland wastewater effluent, sampled on 7/24/13									
Sample Set 1									
7.0	7.7	NA	ND	6	0.1	NA	ND	17.50	243
7.0	7.3	NA	NM	12	0.6	NA	NM	16.90	254
7.0	7.3	NA	NM	18	1.2	NA	NM	16.90	253
7.0	7.3	NA	NM	24	4.1	NA	NM	16.30	256
7.0	7.8	NA	ND	30	6.2	NA	NM	14.80	241
7.0	7.4	NA	NM	36	10.6	NA	NM	15.30	252
7.0	7.3	NA	NM	42	13.5	NA	NM	13.90	253
7.0	7.3	NA	NM	48	21.5	NA	NM	12.80	254
7.0	7.3	NA	NM	54	24.2	NA	NM	11.80	253
7.0	7.6	NA	ND	60	30.5	NA	NM	13.22	244
7.0	7.1	0.5	1.9	NA	1.5	12	1.0	NM	NM
7.0	7.1	0.7	2.5	NA	2.3	18	1.5	NM	NM
7.0	7.2	1.0	3.3	NA	2.9	24	2.0	NM	NM
7.0	7.1	1.2	4.1	NA	3.7	30	2.6	15.30	223
7.0	7.1	1.4	4.5	NA	3.7	36	2.9	NM	NM
7.0	7.1	1.7	5.7	NA	4.6	42	3.5	NM	NM
7.0	7.1	1.9	6.3	NA	5.3	48	3.9	NM	NM
7.0	7.1	2.2	6.7	NA	6.0	54	4.5	NM	NM
7.0	7.1	2.4	7.1	NA	6.7	60	5.1	NM	NM
Sample Set 3									
8.3	8.3	0.2	0.6	NA	2.5	6	2.2	18.40	270
8.3	8.3	0.5	1.1	NA	5.0	12	4.6	19.80	274
8.3	8.3	0.7	2.0	NA	7.4	18	6.7	18.10	269
8.3	8.2	1.0	2.6	NA	9.4	24	8.0	18.90	272
8.3	8.2	1.2	3.3	NA	11.8	30	10.3	18.30	267
8.3	8.2	1.4	3.7	NA	13.4	36	11.9	NM	NM

8.3	8.2	1.7	4.0	NA	15.1	42	14.4	NM	NM
8.3	8.1	1.9	4.9	NA	17.8	48	15.5	NM	NM
8.3	8.1	2.2	5.4	NA	18.8	54	16.3	NM	NM
8.3	8.1	2.4	6.0	NA	19.8	60	17.1	18.5	269

LW – Beaver Lake raw water, sampled on 8/28/13

Sample Set 4

7.0	7.2	NA	NM	4	1.5	NA	NM	NM	NM
7.0	7.2	NA	NM	8	4.5	NA	NM	NM	NM
7.0	7.2	NA	NM	12	8.3	NA	NM	NM	NM
7.0	7.3	NA	NM	16	11.8	NA	NM	NM	NM
7.0	7.2	NA	NM	20	15.3	NA	NM	NM	NM
7.0	7.2	NA	NM	30	26.3	NA	NM	NM	NM
7.0	7.2	NA	NM	40	35.1	NA	NM	NM	NM
7.0	7.4	NA	NM	50	43.1	NA	NM	NM	NM
7.0	7.4	NA	NM	60	56.7	NA	NM	NM	NM
7.0	7.3	NA	NM	80	72.6	NA	NM	NM	NM

Sample Set 5

7.0	7.2	0.1	0.4	NA	0.7	5	0.7	NM	NM
7.0	7.3	0.3	0.6	NA	1.4	10	1.2	NM	NM
7.0	7.2	0.5	1.4	NA	2.6	20	2.2	NM	NM
7.0	7.2	0.8	2.3	NA	3.7	30	3.3	NM	NM
7.0	7.2	1.0	3.7	NA	4.7	40	4.3	NM	NM
7.0	7.2	1.6	5.2	NA	6.9	60	6.2	NM	NM
7.0	7.1	5.2	17.4	NA	14.6	200	12.8	NM	NM
7.0	7.0	9.1	26.2	NA	19.4	350	15.3	NM	NM
7.0	6.9	12.9	32.5	NA	19.9	500	14.4	NM	NM

Sample Set 6

8.3	8.3	0.1	0.4	NA	2.6	5	2.6	NM	NM
8.3	8.3	0.2	0.4	NA	5.2	10	5.1	NM	NM
8.3	8.3	0.2	0.7	NA	7.7	15	7.6	NM	NM
8.3	8.2	0.3	1.1	NA	10.2	20	9.6	NM	NM
8.3	8.3	0.5	1.3	NA	14.4	30	13.9	NM	NM
8.3	8.2	0.6	2.6	NA	19.3	40	18.4	NM	NM

8.3	8.2	1.2	4.8	NA	33.2	75	31.9	NM	NM
8.3	8.1	1.6	6.3	NA	40.1	100	37.6	NM	NM
8.3	7.9	2.4	8.4	NA	52.6	150	50.8	NM	NM
8.3	7.8	3.2	10.1	NA	59.2	200	56.1	NM	NM

WW2 – Noland wastewater effluent, sampled on 9/19/13

Sample Set 7

7.0	7.2	NA	NM	8	0.3	NA	NM	17.90	247
7.0	7.2	NA	NM	16	0.9	NA	NM	17.00	248
7.0	7.2	NA	NM	24	1.5	NA	NM	17.00	254
7.0	7.2	NA	NM	32	4.3	NA	NM	16.80	255
7.0	7.1	NA	NM	40	8.2	NA	NM	16.30	264
7.0	7.1	NA	NM	50	13.3	NA	NM	14.70	255
7.0	7.2	NA	NM	60	18.7	NA	NM	13.30	255
7.0	7.2	NA	NM	80	35.4	NA	NM	10.80	267
7.0	7.2	NA	NM	100	58.3	NA	NM	8.96	271
7.0	7.2	NA	NM	120	73.6	NA	NM	5.68	268

7.0	7.3	0.3	2.0	NA	1.3	10	0.9	15.10	256
7.0	7.2	0.5	2.8	NA	2.8	20	2.3	14.70	252
7.0	7.3	1.1	4.7	NA	4.3	40	4.1	15.00	265
7.0	7.3	1.6	6.2	NA	6.9	60	5.8	14.90	255
7.0	7.3	2.2	9.7	NA	8.3	80	7.0	14.90	255
	7.1	3.3	12.8	NA	11.0	120	9.1	14.70	252
7.0	7.1	5.4	21.0	NA	15.2	200	12.7	14.30	251
7.0	6.9	8.1	30.0	NA	16.9	300	13.7	14.00	252
7.0	6.9	12.2	49.3	NA	18.7	450	14.2	14.00	235
7.0	6.8	18.5	61.3	NA	19.5	680	12.2	13.00	224

Sample Set 9

8.3	8.4	0.1	1.2	NA	1.3	5	1.1	17.00	285
8.3	8.3	0.2	1.9	NA	3.6	10	3.6	17.50	290
8.3	8.4	0.3	2.2	NA	6.0	15	5.8	17.50	287
8.3	8.4	0.4	2.7	NA	8.3	20	7.8	17.80	287
8.3	8.3	0.6	3.5	NA	12.3	30	11.7	17.50	287
8.3	8.3	1.1	5.6	NA	19.2	50	18.8	16.70	287

8.3	8.1	2.1	11.0	NA	34.1	100	33.1	17.10	285
8.3	8.0	3.2	15.2	NA	45.7	150	43.0	16.80	282
8.3	7.8	4.8	22.3	NA	64.5	225	61.4	16.20	280
8.3	7.6	6.4	27.2	NA	66.0	300	63.7	16.20	274

DOC: dissolved organic carbon; Total Ammonia Dose: ammonia added on Day 0; Total Chlorine Dose: free chlorine added on Day 0 measured as total chlorine; Total Monochloramine Dose: theoretical concentration of monochloramine formed based on the total ammonia and total chlorine doses; NM: not measured; ND: not detected; NA: not applicable.

Table 3. Chlorine residuals required to achieve the maximum disinfection byproduct concentration in the formation potential experiments

Disinfection byproduct	FC7	MC7	MC8
	mg L^{-1} as Cl_2		
Trichloromethane	>70	>15	30-60
Dichlorobromomethane	10-40	8-10	>60
Dibromochloromethane	20-60	2.5-3.0	>60
Tribromomethane	1.0-1.2	2.0-3.0	>60
Dichloroacetonitrile	1.5-1.7	>15	>60
Dibromoacetonitrile	1.0-1.2	1.0-1.2	ND

FC7: free chlorine at pH 7.0; MC7: monochloramine at pH 7.0; MC8: monochloramine at pH 8.3; ND: Not Detected

List of Figures

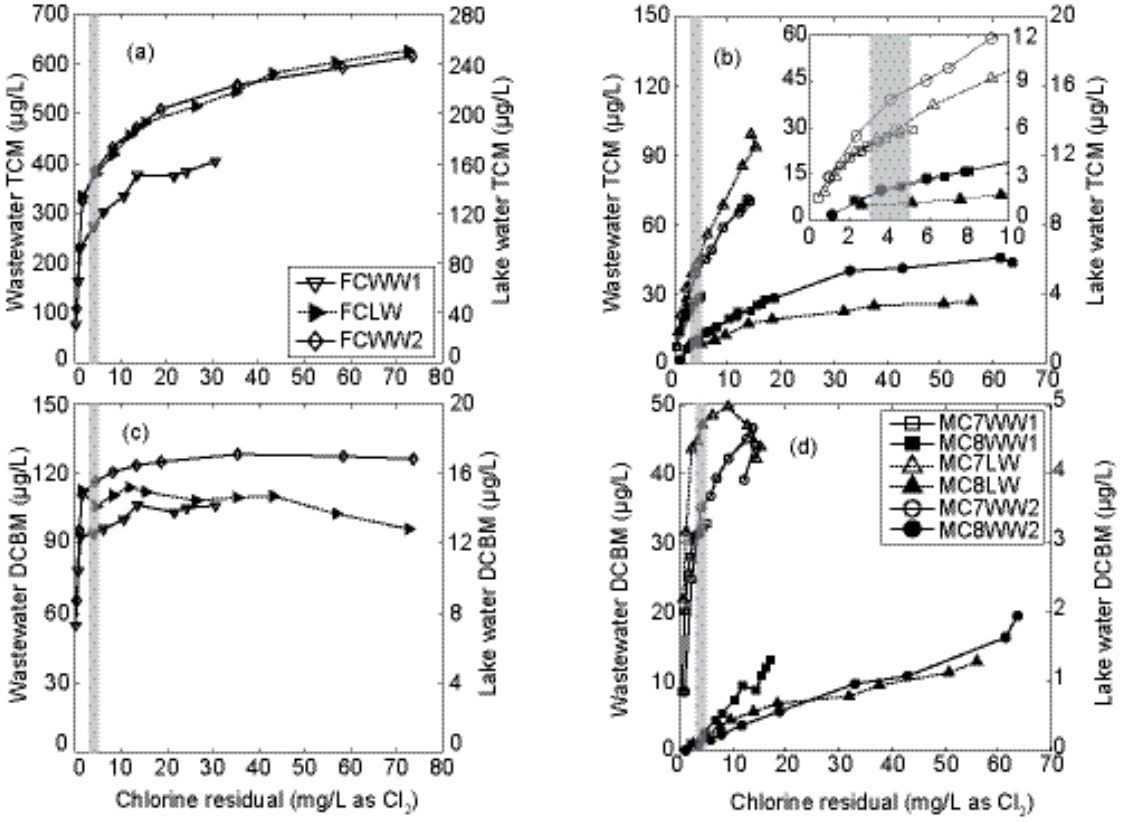

Figure 1 Trihalomethane concentrations versus 7-day chlorine residual (CR) for the three source waters – Noland wastewater effluent collected on 7/24/13 (WW1), Beaver Lake raw water collected on 8/28/13, and Noland wastewater effluent collected on 9/19/13 (WW2). Results of the free chlorine (FC) experiments at pH 7.0 are shown in panels (a), (c), (e), and (g). Results of monochloramine (MC) experiments at pH 7.0 and 8.3 are shown in panels (b), (d), (f), and (h). TCM – trichloromethane; DCBM – dichlorobromomethane; DBCM – dibromochloromethane; and TBM – tribromomethane. Grey-shaded regions are between a CR of 3-5 mg L^{-1} as Cl_2.

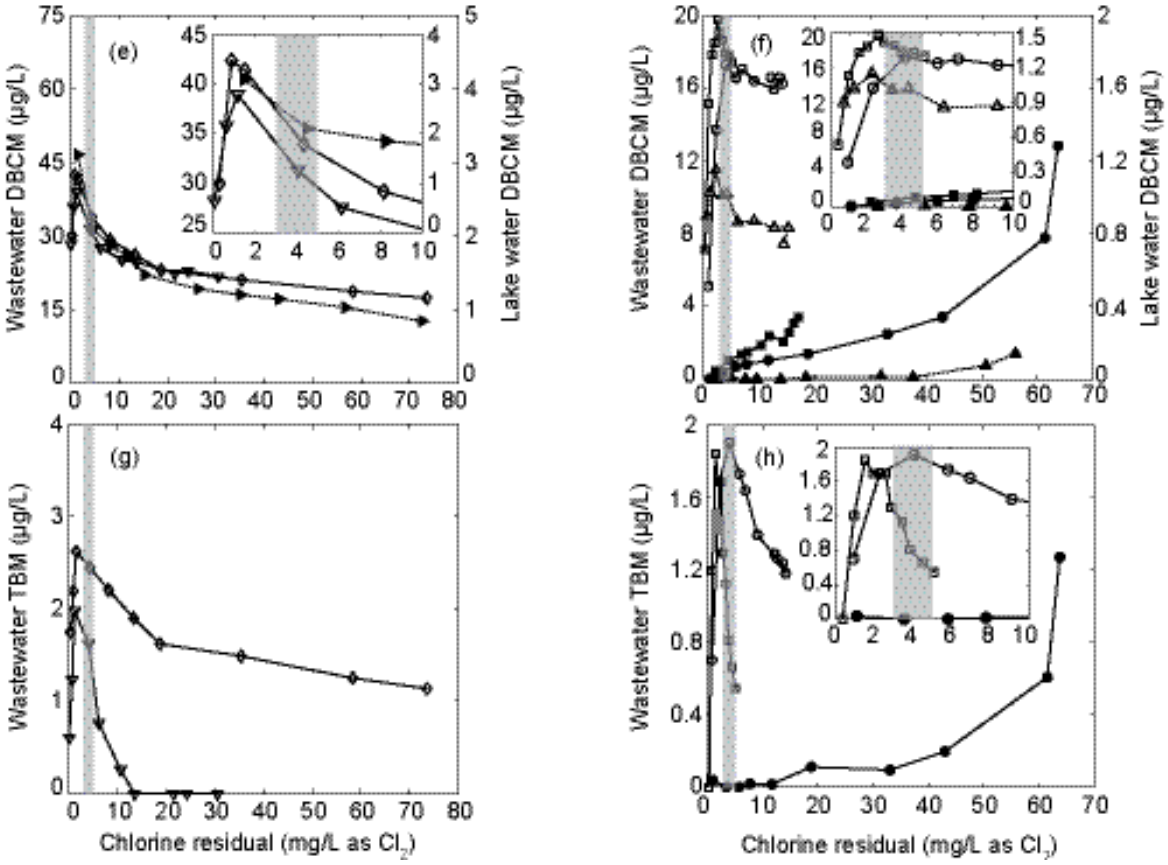

Figure 1 (continue) Trihalomethane concentrations versus 7-day chlorine residual (CR) for the three source waters – Noland wastewater effluent collected on 7/24/13 (WW1), Beaver Lake raw water collected on 8/28/13, and Noland wastewater effluent collected on 9/19/13 (WW2). Results of the free chlorine (FC) experiments at pH 7.0 are shown in panels (a), (c), (e), and (g). Results of monochloramine (MC) experiments at pH 7.0 and 8.3 are shown in panels (b), (d), (f), and (h). TCM – trichloromethane; DCBM – dichlorobromomethane; DBCM – dibromochloromethane; and TBM – tribromomethane. Grey-shaded regions are between a CR of 3-5 mg L^{-1} as Cl_2.

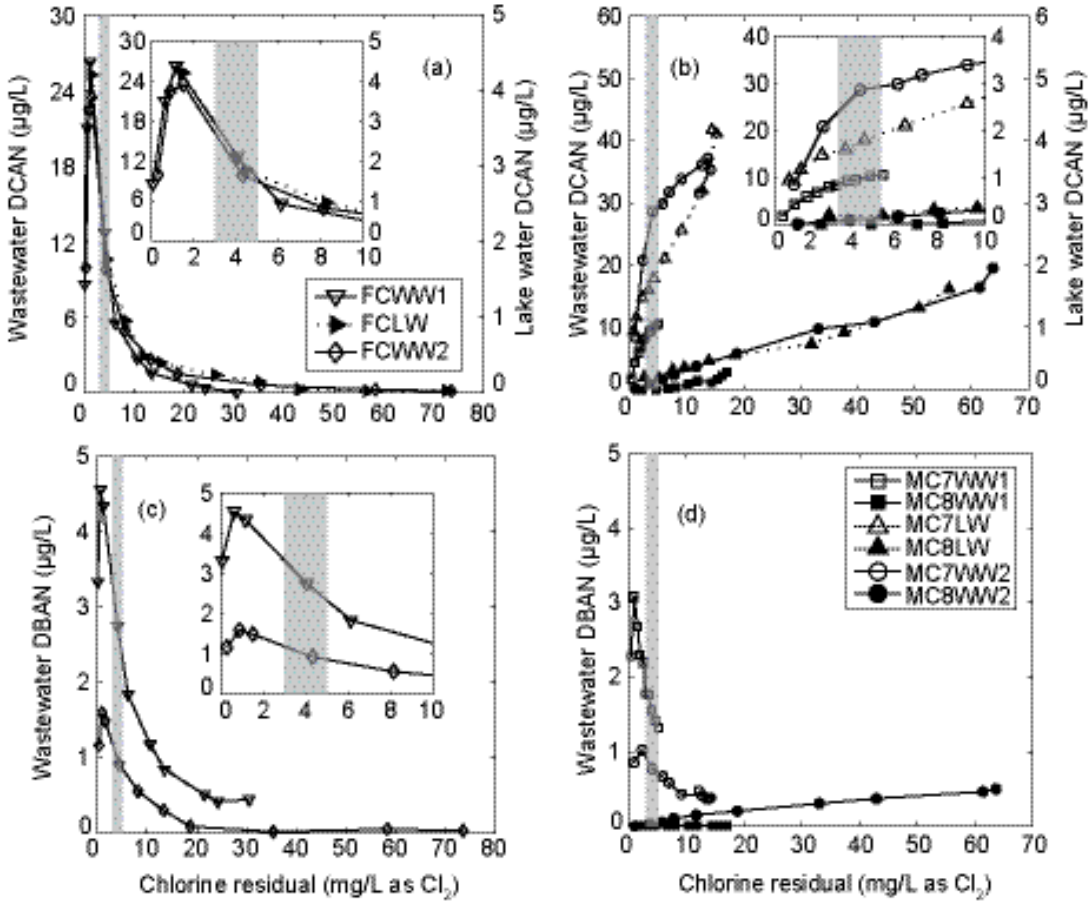

Figure 2 Haloacetonitrile concentrations versus 7-day chlorine residual for the three source waters – Noland wastewater effluent collected on 7/24/13 (WW1), Beaver Lake raw water collected on 8/28/13, and Noland wastewater effluent collected on 9/19/13 (WW2). Results of the free chlorine (FC) experiments at pH 7.0 are shown in panels (a) and (c). Results of monochloramine (MC) experiments at pH 7.0 and 8.3 are shown in panels (b) and (d). DCAN – dichloroacetonitrile; and DBAN – dibromoacetonitrile. Grey-shaded regions are between a CR of 3-5 mg L^{-1} as Cl_2.

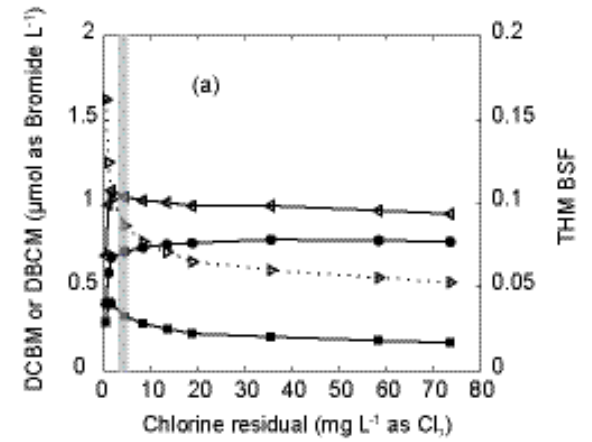

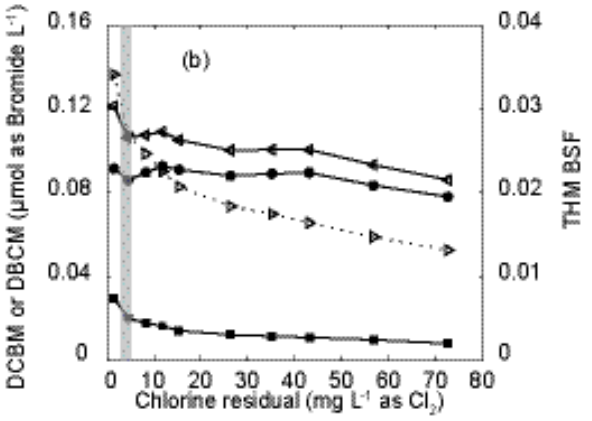

Figure 3 ToTBr FC7

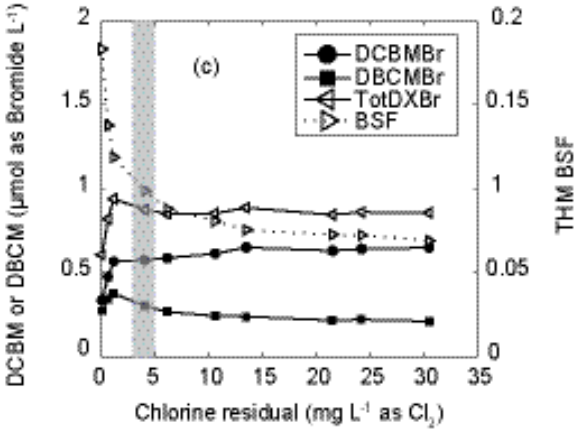

Figure 3 Dichlorobromomethane (DCBM), dibromochloromethane (DBCM), the sum of these two species (TotDXBr), and the trihalomethane bromine substitution factor (THM BSF) as a function of chlorine residual after the 7-day free chlorination period at pH 7.0 for (a) Noland wastewater effluent collected on 7/24/13 (WW1), (b) Beaver Lake raw water collected on 8/28/13, and (c) Noland wastewater effluent collected on 9/19/13 (WW2).

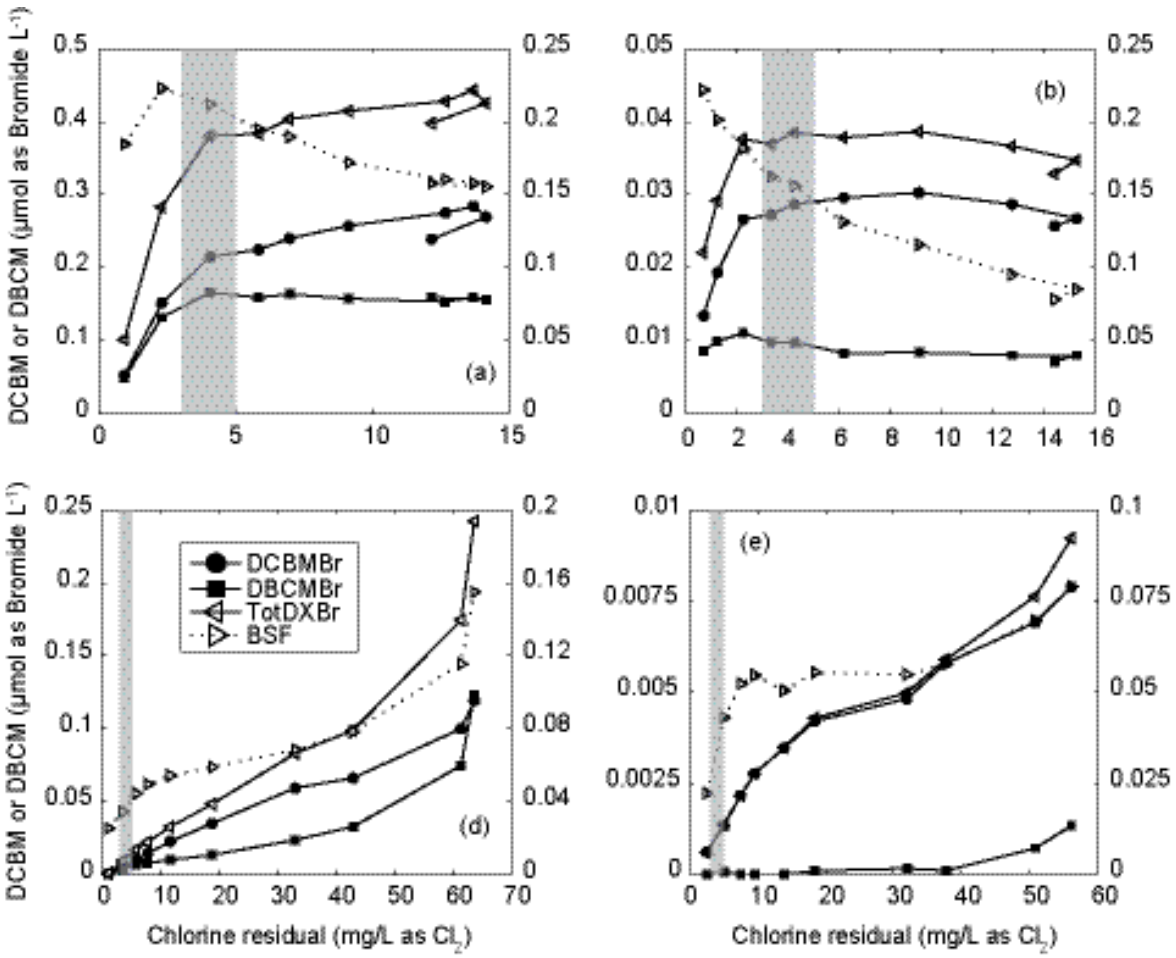

Figure 4 Dichlorobromomethane (DCBM), dibromochloromethane (DBCM), the sum of these two species (TotDXBr), and the trihalomethane bromine substitution factor (THM BSF) as a function of chlorine residual after the 7-day chloramination period at pH 7.0 for (a) Noland wastewater effluent collected on 7/24/13 (WW1), (b) Beaver Lake raw water collected on 8/28/13 (LW), and (c) Noland wastewater effluent collected on 9/19/13 (WW2), and at pH 8.3 for (d) WW1, (e) LW, and (f) WW2. Grey-shaded regions are between a CR of 3-5 mg L^{-1} as Cl_2.

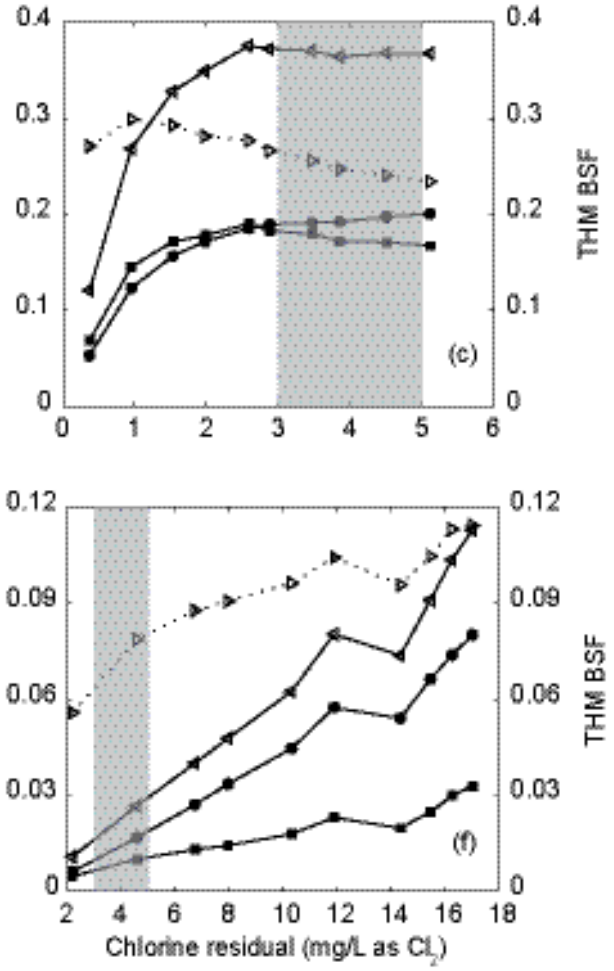

Figure 4 (continue) Dichlorobromomethane (DCBM), dibromochloromethane (DBCM), the sum of these two species (TotDXBr), and the trihalomethane bromine substitution factor (THM BSF) as a function of chlorine residual after the 7-day chloramination period at pH 7.0 for (a) Noland wastewater effluent collected on 7/24/13 (WW1), (b) Beaver Lake raw water collected on 8/28/13 (LW), and (c) Noland wastewater effluent collected on 9/19/13 (WW2), and at pH 8.3 for (d) WW1, (e) LW, and (f) WW2. Grey-shaded regions are between a CR of 3-5 mg L^{-1} as Cl_2.

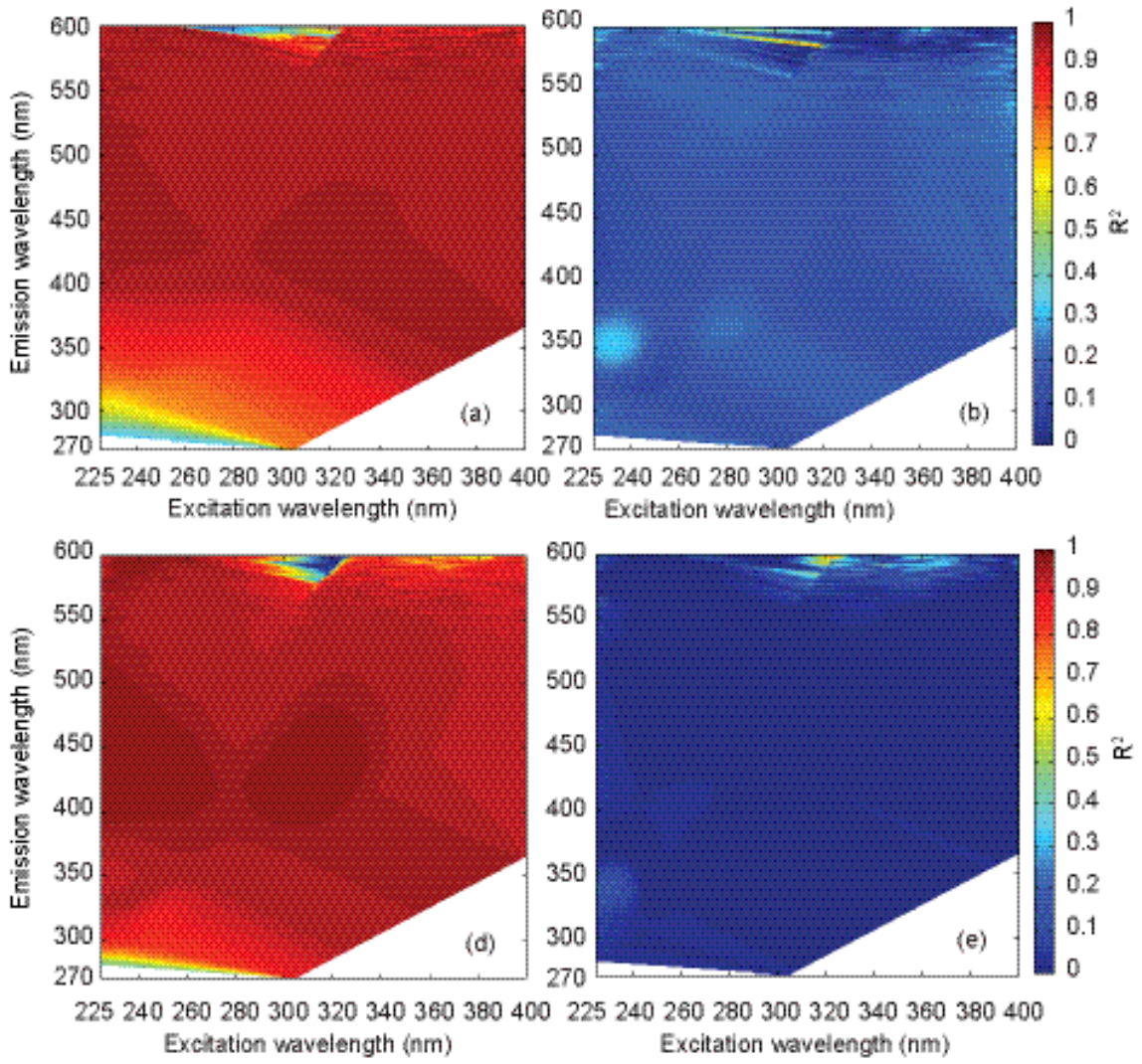

Figure 5 Correlation coefficients (R^2) between trichloromethane formed in the chlorination and chloramination experiments and florescence excitation-emission wavelength pairs, $I_{Ex/Em}$, for (a) free chlorine at pH 7.0 (FC7) with Noland wastewater effluent collected on 7/24/13 (WW1), (b) monochloramine at pH 7.0 (MC7) with WW1, (c) monochloramine at pH 8.3 (MC8) for WW1, (d) FC7 with Noland wastewater effluent collected on 9/19/13 (WW2), (e) MC7 with WW2, and (f) MC8 with WW2.

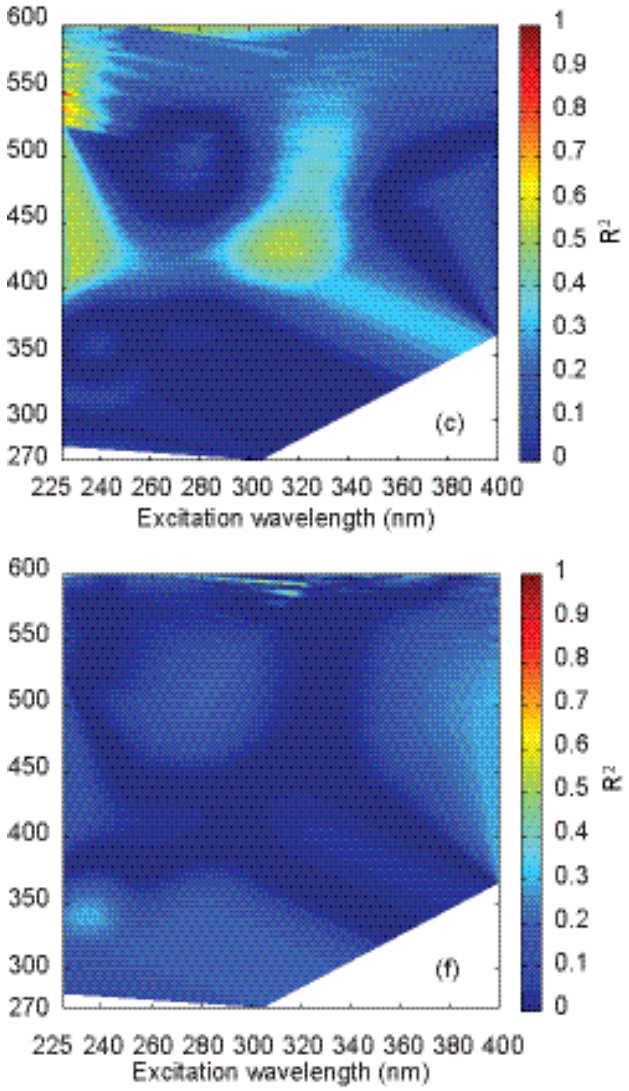

Figure 5 (continue) Correlation coefficients (R^2) between trichloromethane formed in the chlorination and chloramination experiments and florescence excitation-emission wavelength pairs, $I_{Ex/Em}$, for (a) free chlorine at pH 7.0 (FC7) with Noland wastewater effluent collected on 7/24/13 (WW1), (b) monochloramine at pH 7.0 (MC7) with WW1, (c) monochloramine at pH 8.3 (MC8) for WW1, (d) FC7 with Noland wastewater effluent collected on 9/19/13 (WW2), (e) MC7 with WW2, and (f) MC8 with WW2.

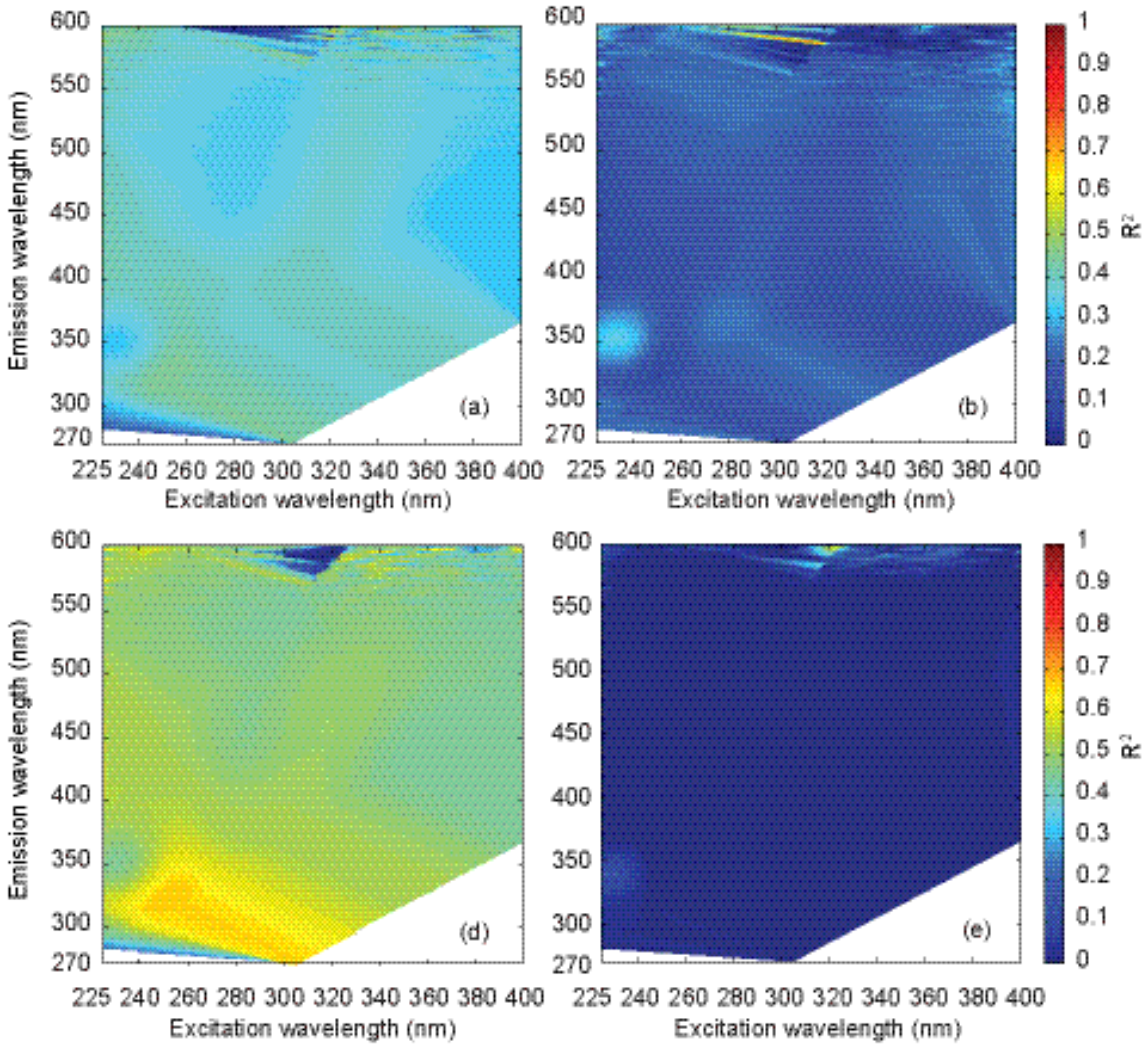

Figure 6 Correlation coefficients (R^2) between dichloroacetonitrile formed in the chlorination and chloramination experiments and florescence excitation-emission wavelength pairs, $I_{Ex/Em}$, for (a) free chlorine at pH 7.0 (FC7) with Noland wastewater effluent collected on 7/24/13 (WW1), (b) monochloramine at pH 7.0 (MC7) with WW1, (c) monochloramine at pH 8.3 (MC8) for WW1, (d) FC7 with Noland wastewater effluent collected on 9/19/13 (WW2), (e) MC7 with WW2, and (f) MC8 with WW2.

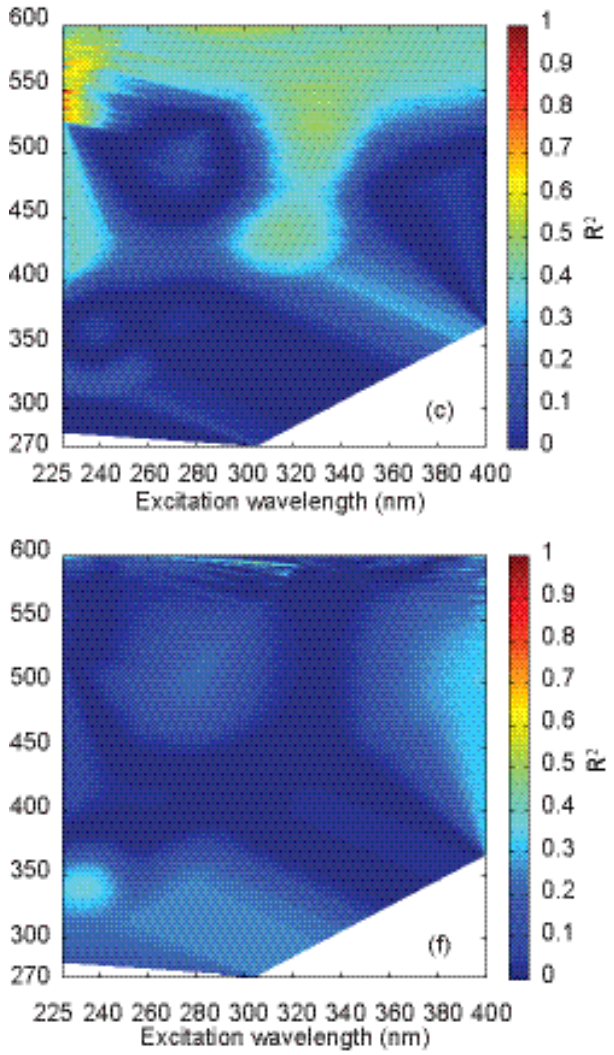

Figure 6 (continue) Correlation coefficients (R^2) between dichloroacetonitrile formed in the chlorination and chloramination experiments and florescence excitation-emission wavelength pairs, $I_{Ex/Em}$, for (a) free chlorine at pH 7.0 (FC7) with Noland wastewater effluent collected on 7/24/13 (WW1), (b) monochloramine at pH 7.0 (MC7) with WW1, (c) monochloramine at pH 8.3 (MC8) for WW1, (d) FC7 with Noland wastewater effluent collected on 9/19/13 (WW2), (e) MC7 with WW2, and (f) MC8 with WW2.

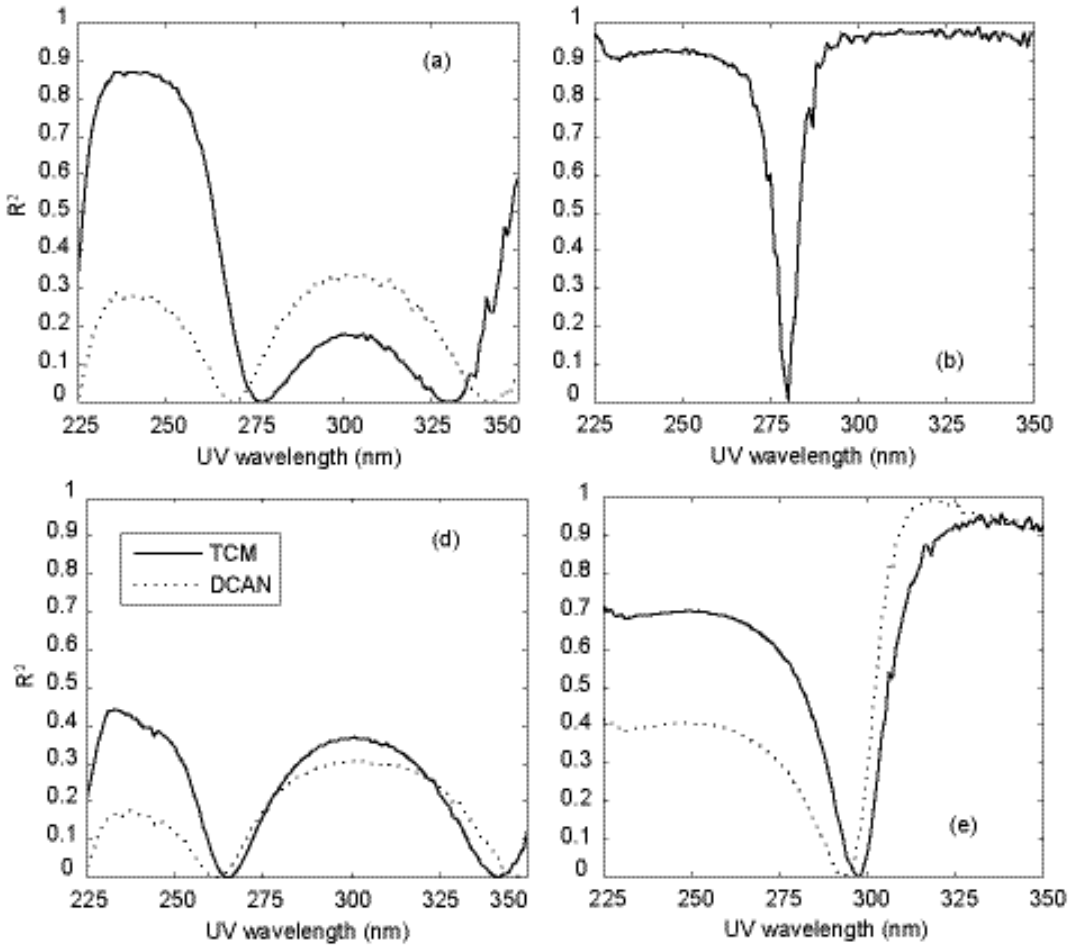

Figure 7 Correlation coefficients (R^2) between trichloromethane (TCM) and dichloroacetonitrile (DCAN) formed in the chlorination and chloramination experiments and ultraviolet absorbance between 225-350 nm for (a) free chlorine at pH 7.0 (FC7) with Noland wastewater effluent collected on 7/24/13 (WW1), (b) monochloramine at pH 7.0 (MC7) with WW1, (c) monochloramine at pH 8.3 (MC8) for WW1, (d) FC7 with Noland wastewater effluent collected on 9/19/13 (WW2), (e) MC7 with WW2, and (f) MC8 with WW2.

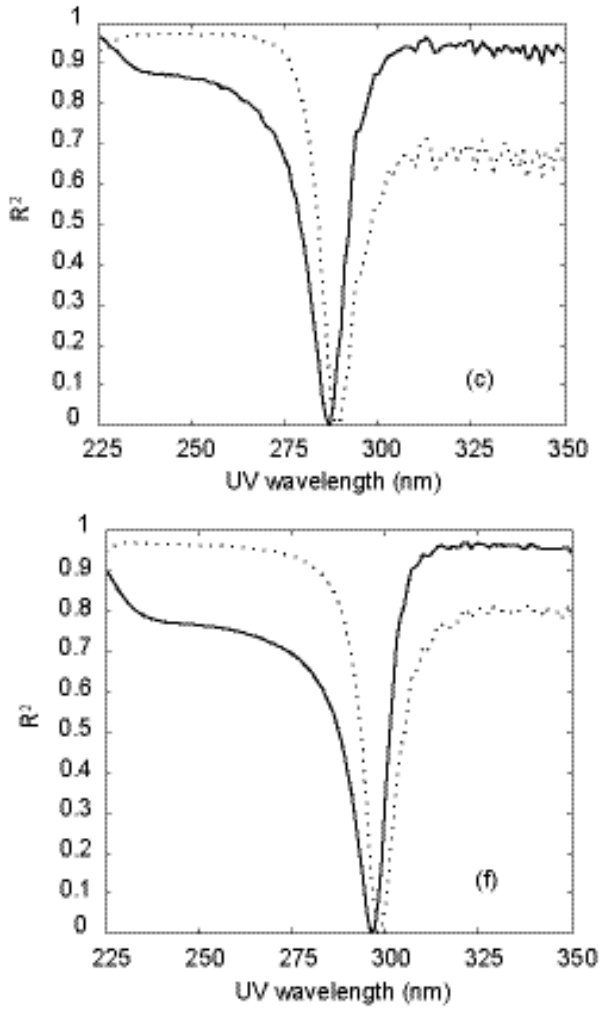

Figure 7 (continue) Correlation coefficients (R^2) between trichloromethane (TCM) and dichloroacetonitrile (DCAN) formed in the chlorination and chloramination experiments and ultraviolet absorbance between 225-350 nm for (a) free chlorine at pH 7.0 (FC7) with Noland wastewater effluent collected on 7/24/13 (WW1), (b) monochloramine at pH 7.0 (MC7) with WW1, (c) monochloramine at pH 8.3 (MC8) for WW1, (d) FC7 with Noland wastewater effluent collected on 9/19/13 (WW2), (e) MC7 with WW2, and (f) MC8 with WW2.